

# Scaffold Fabrication Technologies and Structure/Function Properties in Bone Tissue Engineering

Maurice N. Collins,\* Guang Ren,\* Kieran Young, S. Pina, Rui L. Reis, and J. Miguel Oliveira

Bone tissue engineering (BTE) is a rapidly growing field aiming to create a biofunctional tissue that can integrate and degrade *in vivo* to treat diseased or damaged tissue. It has become evident that scaffold fabrication techniques are very important in dictating the final structural, mechanical properties, and biological response of the implanted biomaterials. A comprehensive review of the current accomplishments on scaffold fabrication techniques, their structure, and function properties for BTE is provided herein. Different types of biomaterials ranging from inorganic biomaterials to natural and synthetic polymers and related composites for scaffold processing are presented. Emergent scaffolding techniques such as electrospinning, freeze-drying, bioprinting, and decellularization are also discussed. Strategies to improve vascularization potential and immunomodulation, which is considered a grand challenge in BTE scaffolding, are also presented.

of interest.<sup>[4]</sup> Bone tissue engineering (BTE) strategies (Figure 1) are showing promise to replace lost or damaged bone tissue, over more traditional bone grafting methods, such as autografts or allografts.

Several scaffold fabrication techniques are at the forefront of tissue engineering (TE), such as electrospinning, freeze-drying, bioprinting, and decellularization.<sup>[6]</sup> Combined with these fabrication methods, a vast array of materials has been selected for BTE. This selection is generally based on functional and biological requirements of bone tissue, which itself is a composite material consisting of inorganic and natural components, organized in a highly hierarchical manner. There has been a recent shift in thinking from

bio-inert materials to bioactive materials, focused on naturally occurring biopolymers due to their inherent ability to interact with growing cells and their ease of chemical modification.<sup>[7]</sup> Recently, biomaterials derived from decellularized extracellular matrix have also been applied in BTE scaffolding. Decellularized bone extracellular matrix (ECM) maintains the native matrix structure, growth factors, and cytokines, thus enhancing cell viability and growth for tissue repair and regeneration.<sup>[8]</sup>


Although a lot of recent research has been conducted on this topic, the selection of fabrication methodologies and different biomaterials for BTE is still grounded in hypothesis with no clear path forward. BTE has been the subject of previous reviews focusing on biomaterials,<sup>[9]</sup> fabrication techniques,<sup>[6a,b,10]</sup> and structural design.<sup>[11]</sup> However, this review focuses on the evaluation of fabrication methodologies for bone scaffolding, while

## 1. Introduction

Tissue engineering aims to develop new biofunctional tissues, to regenerate and repair damaged or diseased tissue. The number of orthopedic surgery procedures performed worldwide totaled approximately 22.3 million in 2017 and is projected to approach 28.3 million by 2022.<sup>[1]</sup> Diseased or damaged bone tissue currently places an enormous demand on bone substitutes for transplantation, being the second most transplanted tissue annually.<sup>[2]</sup> Typically, bone repair is carried out using bone tissue directly from the patient or from compatible donors. These treatments are limited to smaller size defects due to surrounding tissue supply shortage, donor site morbidity, and incompatibility.<sup>[3]</sup> In order to overcome those limitations, fabrication of biomimetic scaffolds is an ever-increasing area

Dr. M. N. Collins, Dr. G. Ren  
Stokes Laboratories  
Bernal Institute  
University of Limerick  
Limerick V94 T9PX, Ireland  
E-mail: maurice.collins@ul.ie; guang.ren@ul.ie

Dr. M. N. Collins, Dr. G. Ren, K. Young  
School of Engineering  
University of Limerick  
Limerick V94 T9PX, Ireland

 The ORCID identification number(s) for the author(s) of this article can be found under <https://doi.org/10.1002/adfm.202010609>.

© 2021 The Authors. Advanced Functional Materials published by Wiley-VCH GmbH. This is an open access article under the terms of the Creative Commons Attribution License, which permits use, distribution and reproduction in any medium, provided the original work is properly cited.

Dr. M. N. Collins  
Health Research Institute  
University of Limerick  
Limerick V94 T9PX, Ireland

Dr. S. Pina, Prof. R. L. Reis, Dr. J. M. Oliveira  
3B's Research Group  
I3Bs – Research Institute on Biomaterials  
Biodegradables and Biomimetics of University of Minho  
Headquarters of the European Institute of Excellence on Tissue Engineering and Regenerative Medicine  
AvePark, Parque de Ciência e Tecnologia, Zona Industrial da Gandra, Barco, Guimarães 4805-017, Portugal

Dr. S. Pina, Prof. R. L. Reis, Dr. J. M. Oliveira  
ICVS/3B's – PT Associate Laboratory  
AvePark, Zona Industrial da Gandra  
Braga, Guimarães 4710-057, Portugal

DOI: 10.1002/adfm.202010609

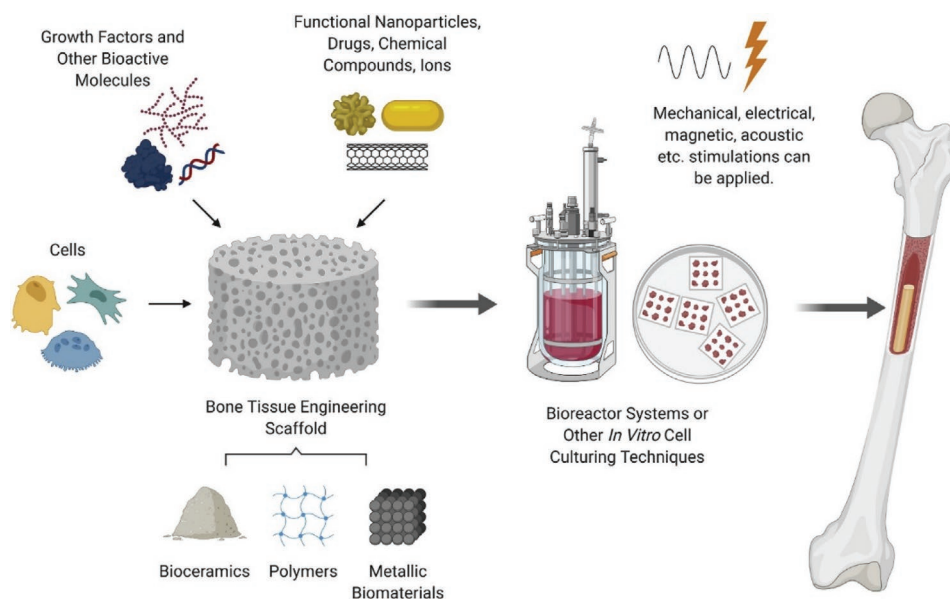


**Figure 1.** Bone tissue engineering strategies. Reproduced with permission.<sup>[5]</sup> Copyright 2020, Elsevier.

providing a commentary for optimum future routes for the fabrication of high-performance bone tissue implants. Specific attention is paid to the mapping of scaffold structure/property/processing relationships to biological function, and how clinical outcomes may be enhanced via concurrent advancements in vascularization, immunomodulation, and osteogenesis.

The first section defines TE in general and BTE in particular. The second and third sections briefly overview the myriad of biomaterials and scaffold fabrication technologies available for BTE. The fourth and fifth sections critically and comprehensively evaluate scaffold structure/property/function relationships for bone tissue engineering while providing a commentary on optimum future routes for the fabrication of high-performance bone tissue implants. This is followed by a discussion of the latest concurrent developments relating to vascularization, immunomodulation, and osteogenesis. Finally,

we provide an outlook for the future while emphasizing the importance of structure/property/function relationships in optimizing clinical outcomes for BTE.

## 2. Biomaterials for Bone Tissue Engineering

Bone is a highly organized composite material comprised by 50–70% inorganic constituents (primarily hydroxyapatite (HAp)), 20–40% organic constituents (primarily type I collagen), 5–10% water, and 3% lipids.<sup>[12]</sup> At a macro-scale, bone can be divided into outer layered hard cortical bone and the spongy trabecular bone.<sup>[13]</sup> Osteoblast cells contribute to the formation of new bone in the form of osteoid, which consists of collagen and other proteins. **Figure 2** illustrates the distribution of these materials respective to their scale within the bone structure.

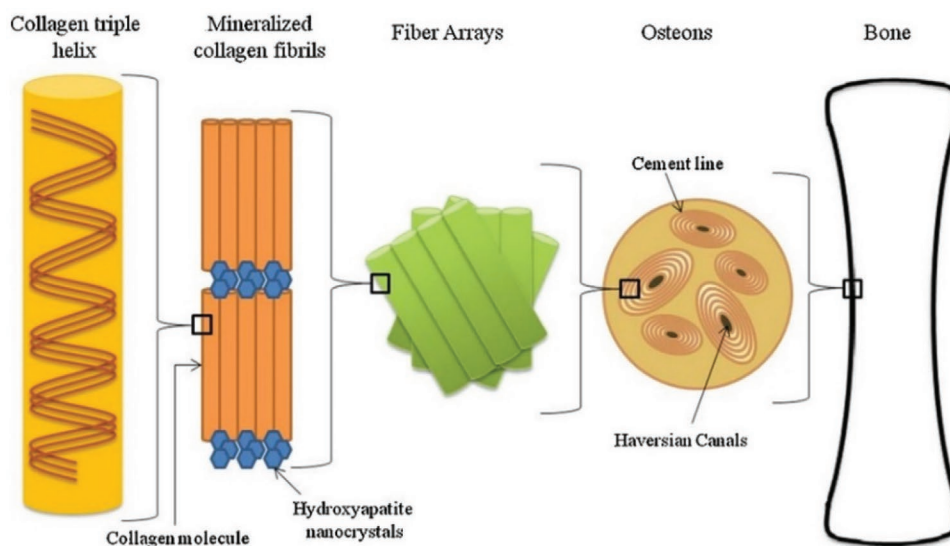


**Figure 2.** Hierarchical organization of bone tissue materials. Reproduced with permission.<sup>[17]</sup> Copyright 2016, Elsevier.

Biocompatibility of materials and their degradation products is also an important consideration in BTE. Scaffolds should allow cell attachment, proliferation, and differentiation, while being non-cytotoxic and evoke minimal immune response.<sup>[5]</sup> For BTE, bioactivity covers two primary biological processes: i) osteoconductivity and ii) osteoinductivity. Osteoconductive scaffolds facilitate bone deposition on the surface of the material in non-osseous sites, while osteoinductive scaffolds employ immature stem cells and direct their differentiation toward bone cells such as preosteoblasts.<sup>[14]</sup>

A wide range of biomaterials have been investigated to bone grafts scaffolding, namely inorganic biomaterials, which comprise metals (e.g., titanium and its alloys) and bioceramics (e.g., calcium phosphates (e.g., HAp and  $\alpha,\beta$ -tricalcium phosphate [ $\alpha,\beta$ -TCP]), calcium carbonates, bioactive glasses and glass-ceramics, alumina, and zirconia), and a myriad of natural (e.g., collagen, gelatin, silk fibroin [SF], chitosan, hyaluronic acid [HA], gellan gum [GG] and derivatives, and alginate) and synthetic polymers (e.g., polyurethanes [PU] and polycaprolactone [PCL]), as well as their combinations (Table 1). Bioceramics are well known for their excellent biocompatibility, osteoconductivity,

and bioresorbability. Polymers have high mechanical strength and stiffness, and benefits are added with natural polymers such as biocompatibility and ECM similarities.<sup>[15]</sup>

The inclusion of cells in fabricated scaffolds is a crucial step in the fabrication process, either during the fabrication process such as 3D bioprinting, or seeding cells on prefabricated scaffolds. Often prefabricated scaffolds are coated with ECM derived gels or ECM-like gels to enhance biocompatibility and to promote cell seeding.<sup>[15,16]</sup>

The implanted biomaterials should provide enough mechanical stability at the time of implantation, while evoking a non-immunogenic response as the biomaterials degrade simultaneously with the growth of native tissue.<sup>[9b]</sup> The biomaterials should also facilitate the proliferation and infiltration of nearby stem cells as well as osteoblast cells. The selection of a biomaterial is driven by the closeness of the mechanical properties to those of native bone tissue. For example, cortical bone has an elastic modulus of 14–20 GPa, while bioactive glass 45S5 Bioglass has a reported elastic modulus of 35 GPa, while PGA reaches 7 GPa and natural biopolymer collagen fibrils  $\approx$ 35 MPa.<sup>[6c,18]</sup> As a result, thermoplastic polymers with higher

**Table 1.** General properties of commonly used biomaterials in BTE.

Material type	Materials	General properties*	Ref.
Inorganic biomaterials—Metals	Titanium and its alloys	High strength, bioinert, low density, not biodegradable, low modulus of elasticity	[20]
Inorganic biomaterials—Bioceramics	HAp	Biocompatible osteoconductive/osteoinductive, brittle, low mechanical strength, slow resorption rate	[21]
	$\beta$ -TCP	Biocompatible, highly resorbable, osteoconductive/osteoinductive brittle	[21a]
	Bioactive glasses	Bioactive, high strength and toughness, elastic modulus, wear resistance, fast degradation rates which can be overcome by incorporating different ions in the glass structure	[18d,22]
	Alumina	High hardness, high abrasion resistance, bioinert, excellent biocompatibility, low fracture toughness, brittle	[23]
	Zirconia	Bioinert, excellent fracture toughness, high strength and elastic modulus, wear resistance, good thermal shock resistance	[24]
Natural polymers	Collagen	Non-cytotoxicity, low antigenicity response, crosslinking capacity, enzymatic biodegradability, complex structure	[25]
	Gelatin	Biocompatible, non-immunogenic, biodegradable, liquefies at physiological temperatures, poor mechanical properties	[25,26]
	SF	Biocompatible, elastic, excellent mechanical strength, slow degradability	[22b,27]
	HA	Biodegradable, biocompatible, viscoelastic Highly hydrophilic, not mechanically stable, slow gelation rate	[28]
	Chitosan	Biodegradable, good antithrombogenic and hemostatic action, mucoadhesion, analgesic effect, antifungal activity, insoluble in water	[21c,29]
	GG	Thermally reversible gel, biocompatible, excellent strength and stability, ionic gelation	[30]
	Alginate	Gelling and viscosity agent, water-uptake ability, biodegradable	[26a,31]
Synthetic polymers	PLLA	Biodegradable, biocompatible	[6c,32]
	PLGA	Biocompatible, biodegradable	[6c,32a]
	PCL	Biocompatible, biodegradable, excellent mechanical properties	[33]
	PU	Biocompatible, biodegradable, good mechanical properties, toxicity of degradation products, slow degradation	[33a,34]
	Inorganic–organic composite biomaterials	SF/ $\beta$ -TCP; SF/HAp; collagen/BCP	Mechanical properties enhancement, high cell attachment and proliferation, increased in vivo response and new bone formation

HAp = hydroxyapatite;  $\beta$ -TCP =  $\beta$ -tricalcium phosphate; SF = silk fibroin; HA = hyaluronic acid; GG = gellan gum; PLLA = poly-L-lactide acid; PLGA = poly-lactic-co-glycolic acid; PCL = polycaprolactone; PU = polyurethane; BCP = biphasic calcium phosphate; \*We include general properties here as the actual properties are influenced by many variables including but not limited to grain size, processing procedure, molecular weight distribution, crosslink density, porosity, etc.

stiffness range and porous bioceramics are often selected for BTE, as they can mimic the load-bearing nature required for bone tissue regeneration.<sup>[19]</sup> The most promising inorganic biomaterials, natural and synthetic polymers used in BTE are described as follows.

## 2.1. Inorganic Biomaterials

Inorganic biomaterials (e.g., metals and bioceramics) have been widely used to repair and regenerate diseased and damaged bone. This type of biomaterials have been particularly applied in bone grafts and cements, orthopedic load-bearing coatings (hip acetabular cups), and periodontal repair.<sup>[36]</sup>

Metallic biomaterials such as titanium and its alloys are characterized by their high strength, low elastic modulus, and low density, while bioceramics have excellent biocompatibility, osteoconductivity, and resistance to corrosion.<sup>[20,37]</sup> Besides, bioceramics are strong in compression but brittle in tension, showing compressive strength of ten times the tensile strength.<sup>[38]</sup>

Among bioceramics, calcium phosphates (HAp and TCP) have long been used due to their resemblance to the mineralogical structure of native bone.<sup>[21a]</sup> TCP, both in its  $\beta$  and  $\alpha$  forms, has high resorption rate, creating a resorbable network, while HAp is the most stable phase under physiological conditions. These materials have limited mechanical strength for load-bearing applications, which can be overcome by combining them with polymers. Besides, this type of ceramics can easily incorporate several bioactive ions, signaling molecules and cells.

Alumina and zirconia are other types of ceramics successfully used in orthopedics, particularly for total hip/knee arthroplasty, owing their chemical bioinertness, and high strength, hardness, cracking, and corrosion resistance.<sup>[23,24]</sup> By combining zirconia and alumina as composites (referred to as zirconia toughened alumina [ZTA]) can improve the low fracture toughness, wear properties, and low susceptibility of degradation of alumina ceramics, thus decreasing the risk of impingement and dislocation, and boosted stability.<sup>[39]</sup>

Bioactive glasses are often used in bone regeneration showing faster capability to bond to connective tissues than other bioceramics, forming a layer of amorphous calcium phosphate or HAp upon implantation.<sup>[6c,18d]</sup> Furthermore, the release of Si, Ca, P, and Na ions from silicate glasses during their dissolution can stimulate osteogenesis and neovascularization/angiogenesis, and enzymatic activity.<sup>[40]</sup>

## 2.2. Natural Biopolymers

Natural biopolymers are especially advantageous in comparison to synthetic polymers, owing their similarity with the ECM, biocompatibility, and biodegradability.<sup>[33a,41]</sup> Biopolymers mostly studied for BTE are proteins (e.g., collagens, gelatin, and SF) and polysaccharides (e.g., chitosan, HA, GG, and alginate). Varying crosslinking strategies are often employed by themselves or in combination with chemical modifications to provide control of scaffold stiffness and structure. These are discussed further in Section 3.3 below.

Collagens and gelatin display similar physical properties and are extensively used across biomedical applications because of their excellent biodegradability, biocompatibility, and immunogenicity.<sup>[42]</sup> Collagens makes up one third of the body's protein being the most abundant polymer found in bone tissue.<sup>[43]</sup> Over more than 29 types of collagen have been documented and are being widely applied in tissue engineering due to its ability for tissue formation and cell growth.<sup>[44]</sup> Across the different types of collagen, type I is the most prevalent in bone tissue, while type II is mostly found in cartilage.<sup>[45]</sup> Recently, collagen derived from marine sources has also attracted attention as an alternative to mammalian collagen, because of its low cost of production and easiness of extractability from the available amount of marine waste residues.<sup>[46]</sup>

Gelatin is a natural water-soluble protein derived from insoluble animal collagen through enzyme processing.<sup>[17]</sup> There are two types of gelatin: Type A that is created via acid treatment, and Type B that is processed with an alkaline, or high pH, solution.<sup>[12]</sup> Nanofibrous scaffolds comprising of gelatin are primarily used in large bone defects repair.<sup>[47]</sup> A host of reasons deem gelatin as a suitable biomaterial for BTE, including: i) biocompatibility and biodegradability; ii) elastic nature; iii) lower antigenicity when compared to parent protein; iv) excellent cell adhesion, and v) accessible functional groups allowing chemical modifications.<sup>[48]</sup> It has also the capacity of gel forming, emulsifying, foaming, and thickening, depending from collagen type, source, and denaturation process. Furthermore, gelatin blends effectively with both natural and synthetic polymers that can promote high bio-affinity and biomechanical properties of the scaffolds.<sup>[47]</sup>

Silk obtained from *Bombyx mori*, mulberry and non-mulberry silks, and spiders, have been the mostly explored in tissue engineering.<sup>[27a]</sup> Particular interest has been given to *B. mori* SF, which is a fibrous protein with a semi-crystalline structure that affords good mechanical strength and stiffness, high biocompatibility, elasticity, and slow degradability. SF is composed by two main crystal structures: i) silk I formed alternatively by  $\alpha$ -helix and  $\beta$ -sheet conformations, and ii) silk II which is an anti-parallel  $\beta$ -sheet structure that contributes to the rigidity and strength of SF.<sup>[49]</sup> The fabrication of SF-based scaffolds is dependent on the control of crystalline/amorphous structure of SF to obtain better mechanical strength, degradation, and aqueous processability.<sup>[27a]</sup>

HA is mostly found in connective tissues and in synovial fluid, and it is characterized by its biodegradability, biocompatibility, and viscoelastic properties.<sup>[28a,b]</sup> Nonetheless, HA has limited mechanical strength, which can be solved by chemical modification or by crosslinking.<sup>[50]</sup>

Chitosan is obtained from the *N*-deacetylation of chitin, and consists of *D*-glucosamine (deacetylated unit) and *N*-acetyl-*D*-glucosamine (acetylated unit) randomly-distributed within the polymer and linked by  $\beta$ -(1-4)-glycosidic bonds.<sup>[51]</sup> It has a polyelectrolyte and cationic nature, good biodegradability, antithrombogenic and hemostatic action, mucoadhesion, analgesic effect, and antifungal activity.<sup>[29a]</sup> GG is a water-soluble and high molecular extracellular polysaccharide, obtained from the organism *Sphingomonas elodea* (originally denominated *Pseudomonas elodea*). It is biocompatible, thermo-responsive with excellent strength and stability, being often used as a gelling agent.<sup>[52]</sup> GG can be obtained in low and high acyl



forms, where low acyl GG forms hard, non-elastic and brittle gels, while high acyl form results in soft, elastic and flexible gels.<sup>[30a]</sup> Alginate, usually found in brown algae cell walls, is seen as a gelling and viscosity agent, with water-uptake ability. Its gelation, biocompatibility, biodegradability, and mechanical strength can be modulated by combining alginate with different bioactive molecules.<sup>[31a]</sup>

### 2.3. Synthetic Polymers

The primary motivation in using biodegradable synthetic polymers is related to their very high strength and stiffness, which is required for bone repair/regeneration. One concern of such type of polymers is that they can undergo a bulk erosion process causing premature failure of scaffolds and even an abruptly release of acidic degradation products that could trigger a strong inflammatory response. However, molecular weight, chemical composition, and crystallinity can be manipulated to allow a controlled degradation rate.<sup>[53]</sup> Poly  $\alpha$ -hydroxy acids, such as PLA, polyglycolic acid (PGA), poly-lactic-co-glycolic acid (PLGA) copolymers, and poly PCL are the biodegradable polymers mostly used in BTE, in part due to their ability of self-reinforcement to achieve a final better strength.<sup>[6c,32a]</sup> Biodegradable polymers typically show less inflammatory response when combined with bioceramics.<sup>[33a]</sup>

PLA is characterized by thermal stability, cytocompatibility, and non-toxic degradation products. It exists in different forms, such as poly-L-lactide acid (PLLA) and poly-D-lactide acid (PDLA), which L/D ratios can be tuned in order to optimize the degradation rate of the materials.<sup>[54]</sup> PLGA, a combination of PGA and PLA, is an FDA approved polymer, with very good biocompatibility, biodegradability, and tunable mechanical properties.<sup>[55]</sup> PCL has also been used in bone repair with FDA approval, is characterized by its good solubility, low melting point, and exceptional blend-compatibility.<sup>[56]</sup> It has good mechanical properties and can be easily processed in comparison to PLA and PGA.<sup>[57]</sup> Particularly, it is very useful for long term implantable devices development, owing its slow degradation rate. The degradation of polyesters is dominated by nonenzymatic hydrolytic scission of ester linkages, therefore PCL can take as long as 3–4 years for complete degradation due to its higher hydrophobicity, while PGA degrades in 1.5–3 months and PLLA degrades in 6–24 months.<sup>[58]</sup> However, its hydrophobic nature is unfavorable for cell attachment and infiltration, which can be solved by combining with different bioceramics and biopolymer coatings.<sup>[59]</sup>

### 2.4. Inorganic–Organic Composite Biomaterials

Inorganic–organic composite materials are a good strategy to mimic the bone tissue, which is itself a natural composite, with mechanical and biological properties significantly better than the single components. An optimal ratio between inorganic and polymeric materials is critical to induce bone tissue formation, while keeping the porosity and mechanical strength of the composites. A wide range of different combinations gives rise to composites with very good performance for BTE.<sup>[27d,29d,35c,g,60]</sup>

For example, using SF combined with  $\beta$ -TCP presented high pore interconnectivity, cell attachment, and proliferation, and adequate in vivo response for BTE.<sup>[35a,b]</sup> Another study have shown that combining biphasic calcium phosphate (BCP) and collagen resulted in higher new bone formation than BCP alone.<sup>[35c]</sup> Furthermore, that authors reported that higher HAp: $\beta$ -TCP proportion in the composites positively influenced new bone formation. For example, inorganic nanoparticles have been also incorporated into polymer matrices to optimize their physical and mechanical properties.<sup>[21e,29d,61]</sup>

## 3. Scaffolding Fabrication Methods

An array of processing techniques has been developed for tissue engineering and consequently, has been applied to BTE (Table 2). Ideally, the optimal fabrication technique can produce repeatable scaffolds with a controlled hierarchal porous structure, as the geometry of the pores structure has profound effects on both mechanical and biological response of bone tissue.<sup>[62]</sup> Nowadays, the fabrication technologies that can facilitate inclusion of cells and growth factors are highly fashionable for optimal scaffold creation.<sup>[63]</sup> It is certain that advanced processing techniques which facilitate the production of highly customizable scaffold geometries for patient specific implants, are required for specialized clinical needs. Current methods for producing bone tissue scaffolds can include: i) electrospinning, ii) freeze drying, iii) 3D printing or additive manufacturing (AM), iv) phase separation, v) gas foaming and vi) particulate leaching (Table 2). Some of these techniques can be broken down into further subcategories, for example AM can be subdivided into fused deposition modelling (FDM), direct ink writing (DIW), stereolithography (SLA), digital light processing (DLP), and selective laser sintering (SLS).

The functionality and operating methods of three most promising techniques for the future are discussed as follows.

### 3.1. Electrospinning

Electrospinning involves a process in which a stream of an electrically-charged polymer in a viscous state or solution is drawn into fiber due to electrostatic forces.<sup>[70]</sup> A basic electrospinning apparatus is comprised of four main parts: i) syringe pump, ii) power supply, iii) metallic needle to allow the electricity to move into the polymeric solution, and iv) metallic collector for fiber collection.<sup>[64b]</sup> A scaffold is typically created by connecting the spinneret and fiber collector to opposite ended electrical terminals. The potential difference between terminals causes the material to be drawn out and deposited onto a collector, which facilitates the fabrication of fibers in the nano scale.<sup>[6a]</sup> Collagen and gelatin nanofibers with high porosities with high surface areas are typically processed via electrospinning.<sup>[71]</sup>

### 3.2. Freeze Drying

Freeze drying or lyophilization, is based on the drying of polymeric solutions. It can be broken down into a three-step process:

**Table 2.** Description, properties, biomaterials, porosity, and structure/processing of typical fabrication methods used for BTE.

Fabrication methods	Description	Biomaterials	Properties	Resolution/porosity	Structure-processing	Ref.
Electrospinning	Use of electrostatic forces to produce fibers	Gelatin, collagen, and PCL	Fast, control over: porosity, fiber diameter, and pore size; Post-fabrication structural details difficult to maintain	100 nm to 6 $\mu\text{m}$ (fiber diameter), 80–95%	Very slow production, reduction in pore size with fiber thickness	[6a,c,7b,9e,12,64]
Freeze drying	Use of a dehydration process to remove solvent from a frozen solution	Natural or synthetic polymers, natural/synthetic-inorganic composites (e.g., gelatin/HA, collagen/HA)	No leaching phase, easy control of porosity; Slow, expensive, and high energy consumption	15–200 $\mu\text{m}$ , 30–90%	Quality of pore interconnection unknown, irregular pore sizes	[6c,7b,12,64,65]
AM: SLS	Layer-by-layer laser curing process	Synthetic polymers, polymer-ceramic/inorganic composites (e.g., PCL/TCP, PLLA/Mg, PCL/HA)	A broad variety of biomaterials, no need for assistance and post-processing; Thermal distortion that can cause shrinking and warping issues	50–100 $\mu\text{m}$	Elevated processing temperatures	[6a,10c,12,64c,66]
AM: SLA	Laser/photo curing of photosensitive resin	Limited materials: epoxy/HA, poly(trimethylene carbonate)/nHA, poly(ethylene glycol-co-depsipeptide) hydrogel	High accuracy, complex 3D structure, cell inclusion; Limited to photosensitive resin; layers cause stair-stepping instead of smooth surface	25–100 $\mu\text{m}$	Challenge balancing biological and mechanical properties for limited materials	[6a,10b,d,64b,c,66a,d,67]
AM: FDM	Layer-by-layer deposition of heated/melted filament	Synthetic polymers (e.g., PCL, PLA, PLGA)	High porosity, complete pore interconnectivity, control over porosity, and pore size; print quality is not as good as SLA or SLS; limited to thermoplastic polymers; problems with warping and minor shrinking	100–150 $\mu\text{m}$	Requires support structures, nozzle clogging	[6a,c,10d,11d,64c,66a–c,68]
Bioprinting	Co-extruded filament with a cell-laden gel to produce a layer by layer construct	Natural and synthetic polymers with inorganic additions (PCL, HA, alginate, SF, chitosan, GelMA, varying cell types)	High porosity, complete pore interconnectivity, control over porosity and pore size; print quality can be difficult to control	100–150 $\mu\text{m}$	Challenge balancing biological and mechanical properties for limited materials. Cells can cause Nozzle clogging.	[31b,69]
Phase separation	Use of thermal energy to induce separation of a polymer solution	Limited material selection across synthetic polymers only	No reduction in molecular activity; Long time to sublime solvent; possible solvent residue; only suitable for a few certain polymer configurations	50–150 $\mu\text{m}$ , 60–98%	Only suitable for thermoplastics, difficulties in monitoring scaffold structure	[12,38,64a,b]
Gas foaming	Use of inert gas, high pressure and freeze drying	Typical BTE natural or synthetic polymers, synthetic-inorganic composites (e.g., PLA/HA, chitosan/HA, PLGA/HA)	Generate structures with a basically unconnected porosity; insufficient mechanical integrity	40–800 $\mu\text{m}$ , <85%	Internal microstructure not explicitly defined, closed pore structure with low interconnectivity	[6a,64b,c,65a]
Particulate leaching	Polymeric solution cast into a mold and solvent removed by lyophilization	Typical BTE natural or synthetic polymers	Salt/polymer ratio can control pore size; possible residues of solvent or salt particles; isotropic structure; insufficient mechanical integrity	30–300 $\mu\text{m}$ , <85%	Nonhomogeneous dispersion of pores, lack of pore inner connectivity, difficulty in fabricating thick scaffolds	[6c,64c,65a]

AM = additive manufacturing; SLS = selective laser sintering; SLA = stereolithography; FDM = fused deposition modeling.

i) solution preparation, ii) casting or molding of the solution, and iii) freezing and drying at low pressure. During the third step, the ice and the unfrozen water are extracted by sublimation and desorption, respectively. Freeze drying is capable of producing scaffolds with approximately 90% porosity and pore sizes ranging from 20 to 200  $\mu\text{m}$ . Pore size is controlled by freeze rate, polymer concentration, and temperature.<sup>[7b]</sup> In order to produce a scaffold with high porosity and interconnectivity a high strong vacuum is required.

### 3.3. Bioprinting

Bioprinting is unique as it creates layered complex and customizable geometries, via 3D digital models produced with the computer-aided design (CAD) software.<sup>[72]</sup> This emerging technology is able to produce geometries with controlled architecture and porosity, tunable structural and mechanical properties, all while being reproducible, and cost-effective. Furthermore, cells, bioactive molecules, and/or drugs can be

incorporated into the structures to yield better cellular response. A diversity of natural and synthetic polymers, bioceramics, and their combinations have been used for bioink production, while collagen and its derivatives are the most commonly used for cell-laden solutions.<sup>[73]</sup>

Bioprinting can be split up into the following steps: i) pre-processing; ii) processing; and iii) post-processing. Pre-processing refers to imaging of the anatomic structure of the target tissue by means of computerized tomography (CT) or magnetic resonance imaging (MRI) scans and translating those images to sliced 3D models.<sup>[74]</sup> The processing step encompasses everything that is involved in the production of the bioprinted tissue, that is, bioink development and scaffold fabrication. Post-processing refers to the maturation of the bioprinted tissue until suitable for in vivo usage, typically taking place in a bioreactor.

Several requirements should be considered for printable bioinks, such as rheological behavior (viscosity and shear thinning), surface tension, swelling, gelation kinetics, and mechanical properties of the materials.<sup>[75]</sup> Another important aspect is the bioinks crosslinking—physical, chemical, or enzymatic—during the processing and post-processing steps, to preserve the biomechanical stability of the printed structures/constructs. Physical crosslinking depends on temperature and molecular interactions to create non-covalent bonds and organic free radical species. Examples of physical crosslinking are the use of divalent ions (e.g.,  $\text{Ca}^{2+}$ ,  $\text{Ba}^{2+}$ , and  $\text{Mg}^{2+}$ ) to crosslink alginate.<sup>[76]</sup> Chemical crosslinking is obtained by the formation of covalent bonds between polymer chains, and it is more stable and stronger than physical crosslinking.<sup>[77]</sup> Glutaraldehyde (GTA), 1-ethyl-3-[3-dimethylaminopropyl] carbodiimide hydrochloride (EDC), and 1,4-butanediol diglycidyl ether (BDDGE) are the most common crosslinkers for functional groups of the polymers (e.g.,  $-\text{COOH}$ ,  $-\text{OH}$ , or  $-\text{NH}_2$ ).<sup>[78]</sup> Enzymatic crosslinking also promotes the covalent bonding between protein-based polymers, with rapid gelation (no more than 10 min) under physiological conditions.<sup>[76]</sup> Diverse enzymes have been used for gelation in situ, such as transglutaminase, sortase, lysyl oxidase, plasma amine oxidase, phosphopantetheinyl transferase, phosphatases,  $\beta$ -lactamase, thermolysin, and peroxidases.<sup>[76,79]</sup> Among them, horseradish peroxidase (HRP) has particular interest for the biomedical field, owing to its fast gelation and controllable crosslinking density. HRP catalyzes the coupling of aniline, phenol and tyramine in the presence of an oxidizer, such as hydrogen peroxide ( $\text{H}_2\text{O}_2$ ).<sup>[80]</sup> One example is HRP/ $\text{H}_2\text{O}_2$  to crosslink SF, when combined with elastin, is proposed as fast-setting bioinks for hydrogels bioprinting.<sup>[81]</sup> Methacrylation of biopolymers is another chemical modification widely applied to tailor their mechanical and biofunctionality. For example, gelatin methacrylate (GelMA) is derived by the reaction of gelatin and methacrylic anhydride in the presence of a photoinitiator (e.g., Irgacure 2959).<sup>[82]</sup>

In scaffold-based (top-down approach) bioprinting, an exogenous biomaterial matrix, such as a hydrogel, is printed and cells are either seeded or printed as part of the bioink.<sup>[83]</sup> Top-down approaches to printing are commonly studied for bone tissue as they are likely to achieve the structure and mechanical performance required for bone.<sup>[84]</sup> SLA, SLS, and FDM are the most prevalent forms of bioprinting used in BTE. In order to overcome challenges such as low cell seeding efficiency and

deficient cellular distribution, biomimetic hydrogels that encapsulate regenerative cells within the external matrix are often used. These hydrogels have shown promising capabilities to fulfil the needs for cell viability, cell anchorage, cell delivery, as well as chemical cues for sustained release of growth factors.<sup>[85]</sup> Cellular printing often adopts a scaffold-free (bottom-up) approach which relies on cell aggregates to fuse together by means of autonomous self-assembly. The techniques used for cellular printing are droplet-based bioprinting (adapted from DIW), extrusion-based bioprinting (adapted from FDM), and laser-assisted bioprinting. Current bioprinting techniques are primarily dominated by single components bioink, which often lack of an acceptable trade-off between cell viability and printer processability.<sup>[86]</sup> These techniques are not suitable for printing large bone scaffolds but for smaller tissue with high cell densities. Interestingly, hybrid approaches have been explored showing promising achievements with respect to simultaneously addressing mechanical and biological functions.<sup>[87]</sup>

### 3.4. Decellularization

Decellularized bone matrix (DBM) has been widely used in BTE as scaffolds and as bioinks for biofabrication, aiming to mimic the native bone microenvironment.<sup>[88]</sup> Decellularization involves the removal of all cells from tissue, while retaining the native ECM composition and its architectural integrity, and its ability to promote cell growth and differentiation. Processing techniques to obtain DBM include surfactants and enzymatic methods (e.g., ethylenediaminetetraacetic acid in combination with trypsin or sodium dodecyl sulfate (SDS) with ammonium hydroxide, Triton X-100, and sodium deoxycholate, and nucleases and proteases), as well as thermal shock, sonication, and hydrostatic pressure.<sup>[89]</sup> The latter has the advantage of no harmful chemical usage and minimization of protein denaturation, thus a high level of ECM content can be preserved.<sup>[90]</sup> Final steps involve the use of nucleases and dehydrated alcohol for a complete removal of cellular remains. Decellularization is confirmed by measuring DNA content and by cell nuclei staining.<sup>[91]</sup>

DBM-based scaffolds can be fabricated by DBM alone or in combination with a variety of polymers and bioceramics to enhance its mechanical performance, osteogenesis, and vascularization potential.<sup>[88b,d,92]</sup>

## 4. Scaffold Structure/Function Properties in Bone Tissue Engineering

Bone tissue architecture is a critical feature in BTE, as structure influences both mechanical properties and biological response. While performing the load-bearing functions of the native bone, the scaffolds should also facilitate vascularization.<sup>[93]</sup> The interconnected porous structure of the scaffolds (**Figure 3**) allows native cells to migrate and proliferate.<sup>[5]</sup> In addition, an optimal design should provide sufficient surface area for cell–scaffold interactions, while facilitating oxygen and nutrient diffusion, as well as the expulsion of waste products.<sup>[94]</sup>

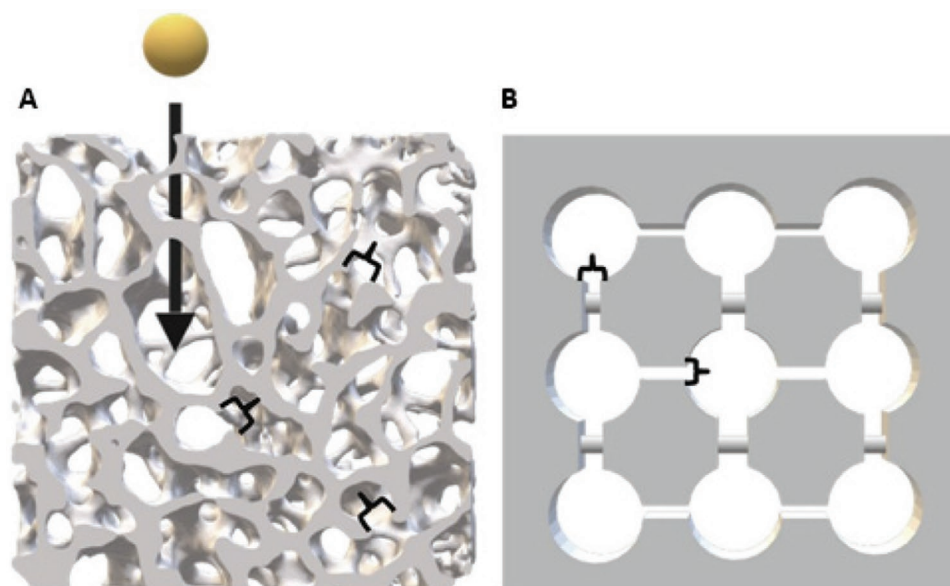


**Figure 3.** Schematic of A) percolation theory and B) bottleneck dimension in a scaffold. Reproduced with permission.<sup>[5]</sup> Copyright 2020, Elsevier.

Typically, a pore size of  $\geq 300 \mu\text{m}$  is required to facilitate new bone formation and vascularization, while the minimum accepted size is  $\approx 100 \mu\text{m}$ .<sup>[95]</sup> Larger pore size proves to be optimal for bone growth due to the sufficient space provided for oxygen and nutrient supply, that further facilitated vascularization in new bone tissue.<sup>[96]</sup> Typically, pore sizes for BTE scaffolding are in the range of 50 to  $>900 \mu\text{m}$ .<sup>[5]</sup> Macropores have been shown to promote osteoinductivity by mediating vascularization.<sup>[97]</sup> However, pore sizes of less than  $100 \mu\text{m}$  may prevent angiogenesis.<sup>[98]</sup> An average pore size of  $550 \mu\text{m}$  has proven to be optimal for bone formation, while hierarchical porous structures have been shown to enhance biological properties.<sup>[5]</sup> Percolation theory, as shown in Figure 3A, is used to calculate the diameter of the largest tracer that can cross the interconnected pores of a scaffold. The percolation diameter is critical for understanding the interconnection of a scaffold as it limits the size of cells and nutrients that can pass through the scaffold.<sup>[5]</sup> The bottleneck dimension, on the other side, indicated by brackets in Figure 3B, describes the diameter of connections between pores. An in vivo study revealed that the optimal pore/bottleneck dimension for bone substitutes is  $700\text{--}1200 \mu\text{m}$  range and therefore, it can be controlled by printing technologies.<sup>[99]</sup>

Tissue engineered bone needs to have sufficient compressive strength to support bodyweight. Typically, the compressive modulus for trabecular bone and cortical bone ranges from up to 2.0 GPa and  $14\text{--}18 \text{ GPa}$ , respectively.<sup>[7b]</sup> The elastic modulus of fabricated scaffolds, on the other hand, also needs to be high enough to maintain its structure in vivo and to facilitate cell growth.<sup>[100]</sup> The degradation rate of the scaffold must match the growth of native ECM, to ensure mechanical support throughout the lifecycle of the scaffold. This is largely dictated by the rate of fluid ingress, which in turn is a function of porosity.<sup>[101]</sup> Therefore, increased porosity positively impacts scaffold degradation at the cost of decreased mechanical properties.<sup>[102]</sup> The typical inverse relationship between porosity and compressive strength for bone tissue scaffolds is demonstrated

in Figure 4. Pore interconnectivity, pore size shape play an important role in the fabrication of an ideal scaffold for bone tissue repair. Considering that the tissue repair rates decrease with age, the scaffold structural design and material selection should be carefully considered.<sup>[7b]</sup>

Bioprinted bone scaffolds can allow the fabrication of engineered tissues with controlled physical and mechanical properties, combining multi-bioink printing, and printing in different layers and gradients.<sup>[63b,88d,104]</sup> For example, mechanically strong ‘cancellous bone-like’ printable implants, containing stem cells encapsulated in PLGA microparticles and controlled-release of programming factors, help the development of novel localized delivery strategies to direct cellular behavior for bone repair.<sup>[104g]</sup>

Regarding the use of dECM-based scaffolds for BTE, ideal microenvironments with instructive biological molecules

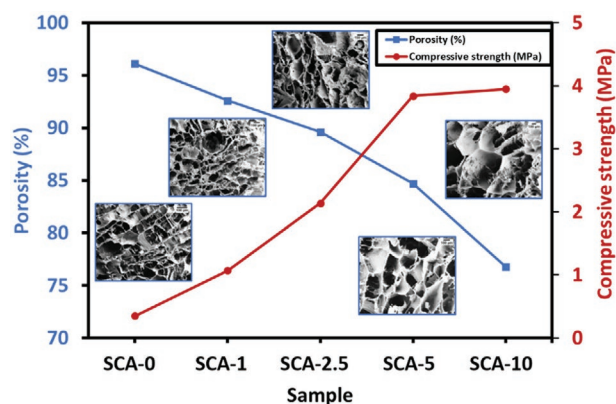


**Figure 4.** Compressive strength, porosity, and morphologies of chitosan/carboxymethyl cellulose (CS/CMC) nano-biocomposite scaffolds, nano-composite scaffolds containing 0%, 1%, 2.5%, 5%, and 10% CCNWs-AgNPs (carboxylated cellulose nanowhiskers decorated with silver nanoparticles) were termed as SCA-0, SCA-1, SCA-2.5, SCA-5, and SCA-10, respectively. Reproduced with permission.<sup>[103]</sup> Copyright 2018, Elsevier.



and reduced immune responses have been reported.<sup>[105]</sup> For example, *in vitro* studies show that rat BMSCs proliferation and differentiation along the osteoblastic lineage on PCL/decellularized bovine small intestinal submucosa/HAP multilayered scaffolds after 21 days of culture, while retaining mechanical performance.<sup>[105b]</sup> Parallel to these studies, bioprinting of dBM-based scaffolds have received considerable attention showing that precise pore size and microporosity can allow tuning of vessel infiltration, which leads to new bone formation, as well as enhanced mechanical stability.<sup>[88d,92c,104d]</sup>

## 5. Scaffold Structure/Processing Relationships in Bone Tissue Engineering

Control of the structure ultimately controls the mechanical properties and to a lesser extent the biological response. Therefore, it is crucial to evaluate which fabrication method can provide the most control over the structure to mimic native tissue. While key aspects of scaffold structure including pore size, shape, orientation, and interconnectivity are directly determined by spatial resolution and geometric control of a processing method, they are indirectly influenced by processing time, crosslinking mechanisms, and thermal degradation. For example, gelation rate is crucial in order to set suitable printing speeds that ensure scaffold stiffness is maintained throughout processing and post processing, therefore gelation of a bioink needs to be analyzed by examining its chemical, physical, or enzymatic crosslinking mechanisms prior to printing.<sup>[106]</sup>

While Table 2 provides insight into the current state-of-the-art fabrication techniques, this does not necessarily provide a simple answer to the question of—which technique will become dominant for BTE? For example, spatial resolution is intrinsically linked with mechanical and biological properties and therefore a key factor, but this needs to be considered within certain context. Comparing additive manufacturing methods, a higher resolution (roughly 15  $\mu\text{m}$ ) can be obtained by inkjet bioprinting of ceramic scaffolds suitable for large bone constructs, however this technique is limited by its incompatibility

with cellular printing. Another example is that cortical bone typically has a porosity of only 5–10%, while cancellous bone contains a porosity of 50–90%, therefore applicable techniques must facilitate creation of porosities across these ranges.<sup>[104e]</sup>

To date no processing technique is capable of constructing architectures identical to that of native bone tissue, however this is expected to be change with the development of advanced health care materials that facilitate micro-extrusion without nozzle clogging, which will provide high levels of spatial resolution.<sup>[104e]</sup> Other processing issue and limitations are likely to be resolved through combining techniques, as for example AM, which can be combined with particulate leaching or freeze drying to overcome the material or structural based limitations.

### 5.1. Clinical Trials

It is worth noting that an optimal biomaterial has yet to be established for BTE, therefore a comparison across fabrication techniques still lacks the merit of a likewise comparison across optimal bone tissue materials. So far, limited bone tissue scaffolds have made their way into the clinical use, while this fails to provide key insights to the structure-processing relationship, it provides a meaningful context with regards to optimal material selection. Zeng et al.<sup>[107]</sup> reviewed studies of clinical trials for the repair of bone defects, eight of which used natural scaffolds (collagen and gelatin) and twelve focused on synthetic scaffolds. It was reported that combining scaffolds with bone stimulating agents expedited bone healing, with HAp/collagen showing the highest grade of bone regeneration. Among few clinically available products, composites that consist of natural biopolymers (both collagen and gelatin) and inorganic additives such as TCP and HAp tend to dominate the market.<sup>[17]</sup>

### 5.2. Hierarchical Structures

As shown in **Figure 5**, since bone regeneration is conducted by the synergistic effect of cells and scaffolds, numerous studies

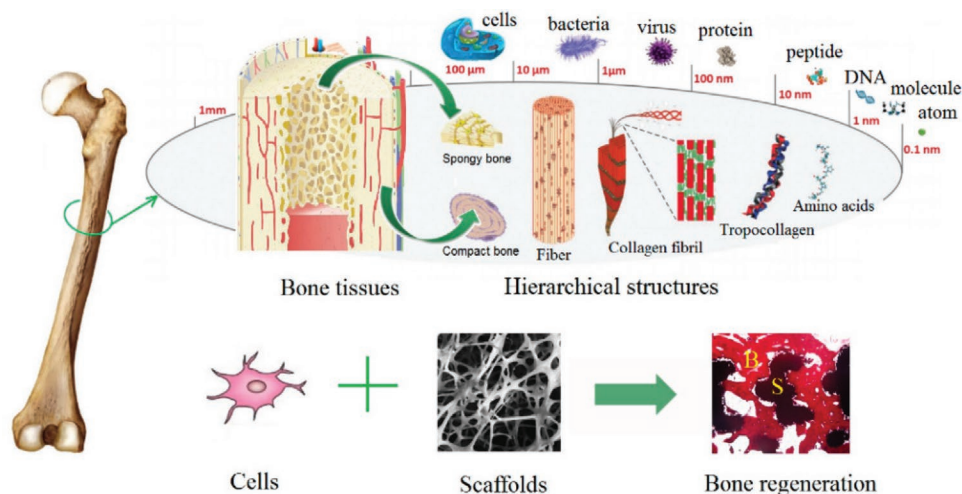


**Figure 5.** The hierarchical pore structure of bone tissue. Reproduced with permission.<sup>[62c]</sup> Copyright 2018, MDPI.

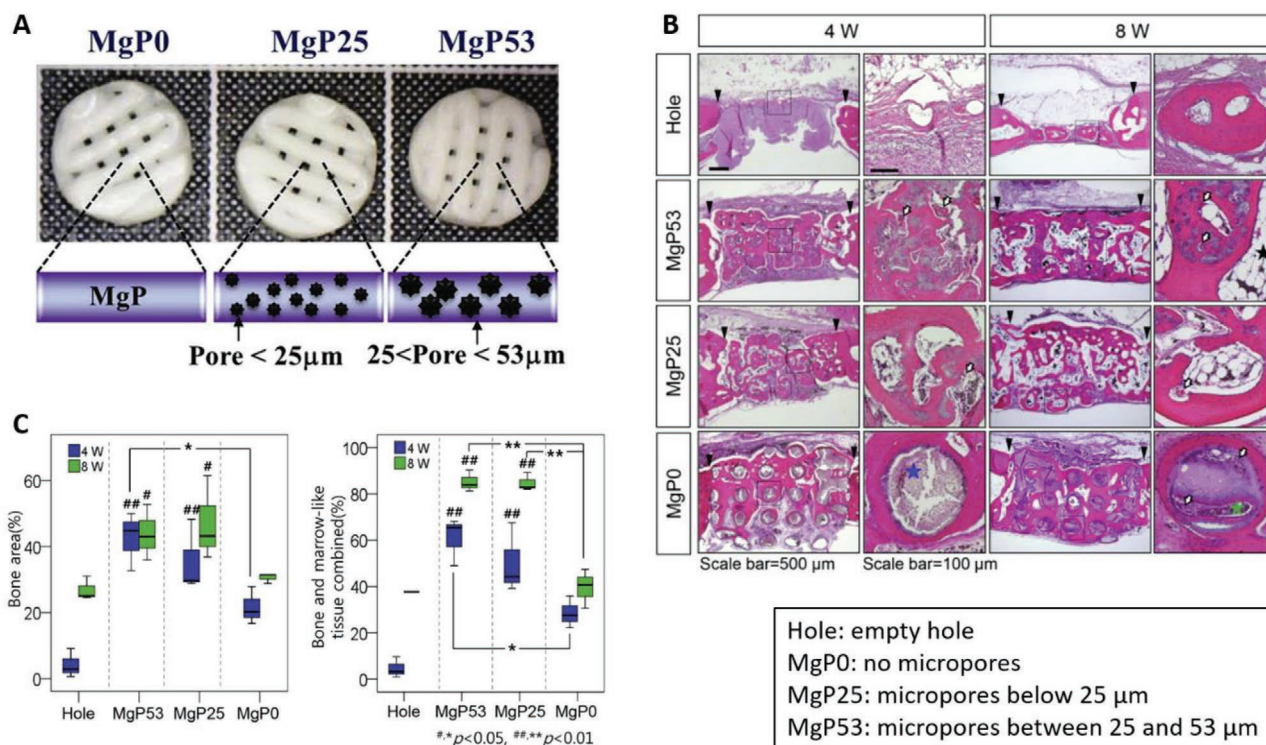


**Figure 6.** Effect of the biodegradation rate controlled by pore structures in magnesium phosphate (MgP) ceramic scaffolds on bone tissue regeneration in vivo: A) MgP scaffolds with varying micropore sizes; B) MgP scaffolds were implanted in the rabbit calvarial defect area (4 mm), and the calvarias were decalcified, sectioned, and stained with hematoxylin and eosin (H&E) after 4 and 8 weeks; C) Bone area and “bone + marrow-like tissue” area at 4 and 8 weeks post-surgery, \* $p$  < 0.05, \*\* $p$  < 0.01. # $p$  < 0.05, # $p$  < 0.01 versus hole group. Reproduced with permission.<sup>[112]</sup> Copyright 2016, Elsevier.

in BTE have adopted the strategy of mimicking the hierarchical pore structures of bone tissues.<sup>[62c,104b,108]</sup> Using a combined method of indirect 3D printing and freeze-drying, created a hierarchical 3D bioactive scaffold that consisted of SF and bioactive glass, which exhibited two levels of pores in the order of 500–600 and 10–50  $\mu$ m. This yield an excellent mechanical stability and flexibility, that the hierarchically porous scaffold did not exhibit any fluctuation after compression loading in a wet condition. Moreover, the biocomposite scaffold promoted the attachment of human bone marrow stem cells, as well as the alkaline phosphatase (ALP) activity as compared to plain SF scaffold, highlighting the promise of hierarchical structures in BTE applications.<sup>[104b]</sup>

Complex morphologies which better mimic the native bone tissue tend to have greater mechanical properties. For example, PCL/PLGA scaffolds show varying Young’s moduli for different scaffold morphology: diagonal (9.81 MPa), staggered (7.43 MPa), and lattice (6.05 MPa).<sup>[109]</sup> A less reported structural feature, which has a distinct and measurable effect on mechanical properties, is pore orientation. This has been examined on chitosan and gelatin (type B) scaffolds fabricated by sequential unidirectional freezing. It was found that compressive, tensile, and shear moduli all show the same trend based on pore orientation, that vertical > random orientation > horizontal.<sup>[110]</sup> This further adds speculation to the processing technique that can create scaffolds with controlled pore orientation aligned to that of the native bone tissue. These efforts have concentrated on combining AM with other traditional tissue engineering approaches such

as gas foaming<sup>[111]</sup> and these methods have shown porosity and geometrical control can be achieved simultaneously.

Kim et al.<sup>[112]</sup> fabricated magnesium phosphate (MgP) ceramic scaffolds of varying pore sizes (macro and micro) using a combination of 3D printing and salt-leaching and investigated the in vivo response in rabbit calvarial model. Three types of scaffolds were created, all with macropores (>100  $\mu$ m) present but varying levels of micropores (Figure 6A). MgP scaffolds containing micropores show a lamellar morphology with higher porosity (Figure 6B), which promotes faster biodegradation that appears to enhance bone formation and remodeling activities, when compared to MgP0 (Figure 6C).

Liu et al.<sup>[113]</sup> reported the impact of differing levels of pores on vascularization in adult rabbits, using poly(3-hydroxybutyrate-co-3-hydroxyhexanoate) (PHBHHx) scaffolds fabricated by combined solvent-casting and particulate leaching methods. While previous studies have primarily looked at porous structures at a macro- and micro-level, Liu et al. demonstrated the ability of mesoporous materials (2–50 nm) to: i) stimulate the formation of HAp, ii) promote proliferation and differentiation of osteoblasts, and iii) increase bone-matrix interface strength. Furthermore, the incorporation of mesoporous materials was beneficial for delivering growth factors such as BMP-2 and promotes angiogenesis which further enhanced bone regeneration, as depicted in Figure 7.

While most fabrication techniques covered in this review are capable of producing a combination of micropores and macropores, increased spatial resolution and accuracy are

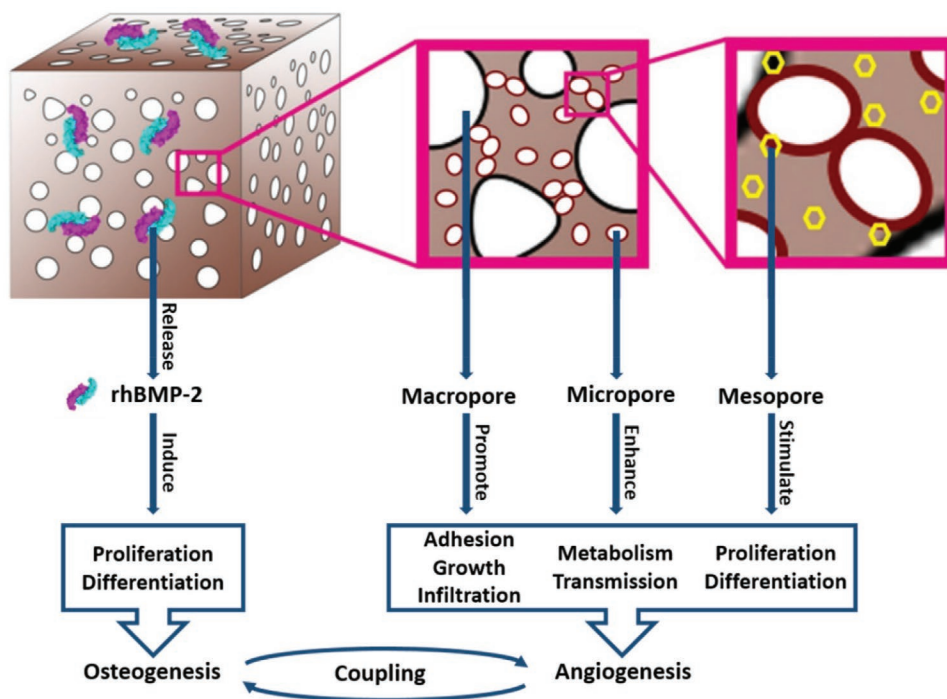


**Figure 7.** Schematic diagram of the effects of scaffold hierarchy on the bone regeneration. Reproduced with permission.<sup>[113]</sup> Copyright 2020, Elsevier.

required to consistently produce highly controlled mesopores. Zheng et al.<sup>[114]</sup> demonstrated the application of metal injection molding (MIM), a near-net forming fabrication method, on the fabrication of titanium implants. This facilitates accurate representation of the porous structure of native bone tissue, down to the mesopore level, and this has proved to be beneficial in *in vivo* osteogenesis canine models. Although titanium, as a bio-stable and bioinert material, used for long-term implantation, is largely out of scope for this review, this manufacturing technique still provides insight on the benefits of precise control over structure in BTE.

## 6. Advanced Strategies for Improving Vascularization of Scaffolds in Bone Tissue Engineering

Vascularization is the most crucial challenge in BTE, since tissue thickness limits nutrient and oxygen diffusion, which is required to support osseointegration and osteogenesis during bone healing and regeneration (Figure 8).<sup>[115]</sup> Angiogenesis is known to influence osteogenesis, where bone progenitor cells and osteoblasts are near vascular endothelial cells during new bone formation, particularly in critical-sized defects.<sup>[116]</sup> Vascular endothelial growth factor (VEGF) is the major growth factor for vascular growth and it is required to effectively couple angiogenesis with osteogenesis during bone repair/regeneration.

Various strategies to develop an appropriate vascular network in engineered scaffolds have been explored, namely: i) use of biocompatible materials in scaffold design; ii) micro-nano structure, morphology, and porosity, and roughness of the scaffolds, as described in Section 5; iii) ion-doped

materials; iv) addition of angiogenic growth factors (e.g., VEGF and fibroblast growth factor (FGF)) or recombinant proteins; and v) co-culture cell systems in static and dynamic conditions (Table 3).<sup>[104c,f,118]</sup>

The fabrication of  $\beta$ -TCP and osteogenic peptide (OP) containing water/PLGA/dichloromethane (DCM) emulsion inks scaffolds using cryogenic 3D printing was reported as vascularization approach for BTE.<sup>[104f]</sup> Scaffolds were then coated with angiogenic peptide (AP) containing collagen type-I hydrogel to ensure angiogenic capability (Figure 10A). *In vitro* angiogenesis tests using rat endothelial cells (ECs) seeded on the scaffolds showed a viability of 98% with alive cells after 3 days of culture (Figure 10B-a,b). It was also observed enhanced EC migration on the extracts of the scaffolds containing AP, due to its fast release (Figure 10B-c,d).

The strategy involving the incorporation of bioactive ions (e.g., Mg, Ce, and Cu) in the materials led to increased levels of angiogenic and osteogenic markers.<sup>[104c,120]</sup> Gu et al.<sup>[104c]</sup> prepared Mg-doped  $\beta$ -TCP scaffolds cultured with human bone marrow mesenchymal stem cells (hBMSCs) and human umbilical vein endothelial cells (HUVECs) to achieve bone formation and favorable vascularization potential. Also, Ma et al.<sup>[120a]</sup> reported a significantly improvement of vascularized bone formation on Mg-doped 3D-printed tantalum scaffolds. Another reported approach is the incorporation of Ce nanoparticles in PLLA/gelatin composite scaffolds obtained through electrospinning.<sup>[120b]</sup> Chick embryo chorioallantoic membrane (CAM) as an *in vivo* model system for angiogenesis evaluation showed a considerable increase of embryonic blood vessels, when treated with VEGF. Another way to deliver bioactive ions with crucial role in vascularization and osteogenesis, is by using bioactive glasses biomaterial scaffolds.<sup>[120d,124]</sup> The release



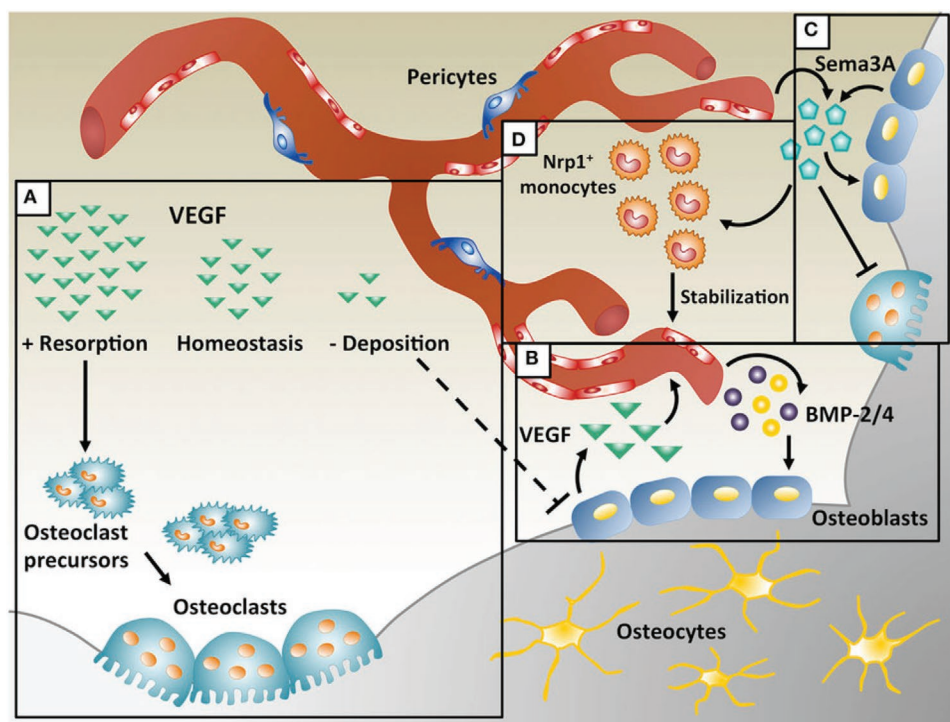


**Figure 8.** Angiogenesis coupled with osteogenesis during intramembranous ossification: A) Physiological levels of vascular endothelial growth factor (VEGF) maintain bone homeostasis. Low VEGF interrupts osteoblast differentiation and high VEGF increases osteoclast recruitment, leading to bone resorption; B) Migration and proliferation of endothelial cells during bone repair, and secretion of bone morphogenetic protein (BMP)-2 and BMP-4; C) VEGF dose dependently regulates Sema3A expression in endothelial cells and Sema3A from different sources suppresses osteoclast differentiation and stimulates bone deposition; D) Sema3A is also responsible for the recruitment of neuropilin 1-expressing (Nrp1+) monocytes, promoting vessel stabilization. Reproduced with permission.<sup>[117]</sup> Copyright 2017, Frontiers Media SA.

of ions presented within bioglasses chemical structure, during network dissolution, can activate different genes associated with vascularization and bone formation.<sup>[125]</sup>

Co-culture of angiogenic cells with pluripotent stem cells has positive effects on new blood vessels formation and osteogenesis, as another vascularization strategy.<sup>[118b,122]</sup> For example, He et al.<sup>[118b]</sup> observed that ASC/endothelial progenitor cells (EPCs) co-culture system combined with HAp scaffold significantly promoted regeneration and angiogenesis of critical-sized bone defects. In a study by Honda et al.,<sup>[122a]</sup> HAp-fiber scaffolds combined with connective tissue growth factor (CTGF), under

co-culture of HUVECs and MC3T3-E1 cells, exhibited enhanced osteogenesis via stimulation of angiogenesis. Thrivikraman et al.<sup>[122b]</sup> developed a cell-laden collagen hydrogel, encapsulating co-culture of HUVECS and BMSCs, able to stimulate the osteogenic differentiation of hMSCs, while enabling the formation of hMSC-supported vascular capillaries in vitro and in vivo. Markou et al.<sup>[122c]</sup> fabricated vascularized tissue using endothelial cells, smooth muscle cells and pericytes (vascular organoids) embedded in collagen/fibrinogen/fibronectin hydrogels, useful as a starting point for capillary-like structures sprouting in vitro and a fast creation of a functional vascular network in vivo.

**Table 3.** Vascularization strategies for BTE.

Strategies	Outcomes	Schematic representation	Ref.
Scaffold architecture	Cellular adhesion, proliferation, and differentiation	Figure 9A	[119,113]
Biomaterials incorporating bioactive ions	Activation of different genes related with vascularization and bone formation	Figure 9B	[104c,120]
Angiogenic growth factors	Short-term with burst release profiles; VEGF initiates macrophage-related angiogenic response in the inflammation stage; FGF, TGF, BMP, IGF, PDGF, and erythropoietin, growth hormone can induce angiogenic response to injury	Figure 9C	[118c,121]
Co-culture systems in static and dynamic conditions	MSCs/ECs enhances the formation of capillary-like structures; Smooth muscle cells facilitate vessel stabilization	Figure 9D	[118b,122]

BMP: bone morphogenetic protein; ECs: endothelial cells; FGF: fibroblast growth factor; HGF: hepatocyte growth factor; IGF: insulin-like growth factor; MSCs: mesenchymal stem cells; PDGF: platelet derived growth factor; TGF: transforming growth factor; VEGF: vascular endothelial growth factor.



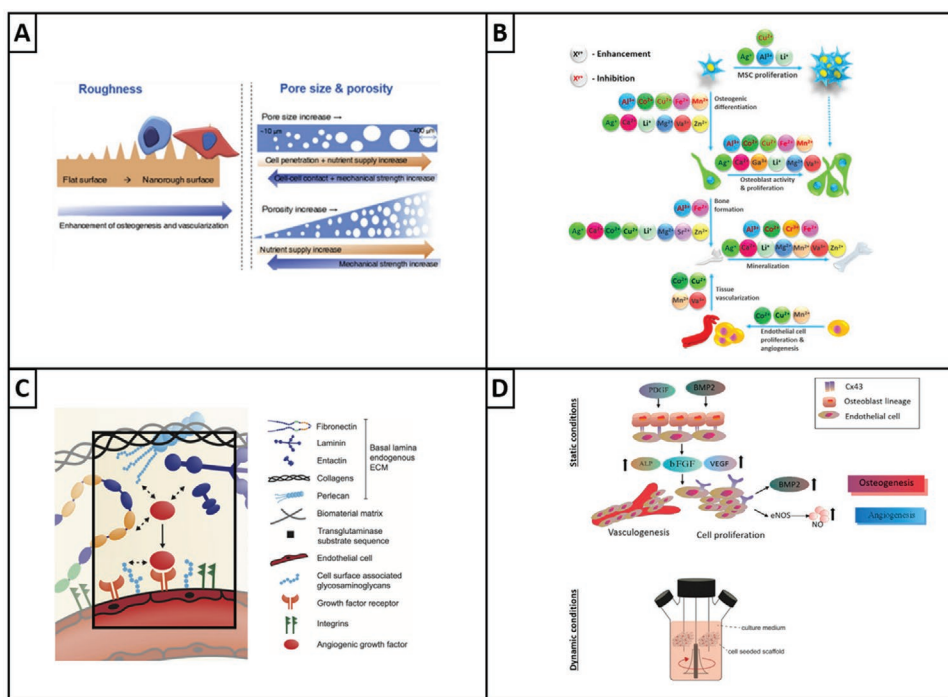


**Figure 9.** Schematic representation of vascularization strategies: A) Scaffold architecture; B) Biomaterials incorporating bioactive ions; C) Angiogenic growth factors; D) Co-culture systems in static and dynamic conditions. Reproduced with permission.<sup>[119,123]</sup> Copyright 2018, Elsevier; 2018, MDPI; 2015, Frontiers Media SA; 2020, Elsevier; 2018, BMC.

A different strategy aiming to reproduce an autologous vascularized BTE were designed using PCL nanofibers (NFM) comprising bound endogenous bone morphogenetic protein-2 (BMP-2) and VEGF on their surface.<sup>[118c]</sup> Chick CAM in vivo assay have showed high mature blood vessels with highly branched capillary network formed in the systems containing endogenous VEGF (VEGF and BMP2|VEGF), after 7 days of implantation (Figure 11).

## 7. Immunomodulatory Scaffolds in Bone Tissue Engineering

Scaffolds with ability to regulate host-to-scaffold immune response with immunomodulatory properties can employ a regenerative potential to a varied extent.<sup>[126]</sup> The activation of immune cells is important in regulating the balance of bone reconstruction and resorption in pathological conditions.<sup>[127]</sup> Among immune cells, macrophages are responsible for phagocytosis and recruitment of other cells crucial in the tissue healing process.

The physicochemical properties of the biomaterials, such as shape, size, porosity, and chemical functionality, as well as the type of biomaterial, can stimulate the immune or inflammatory pathways,<sup>[128]</sup> and ultimately to facilitate new bone formation.<sup>[129]</sup> Wang et al.<sup>[126c]</sup> fabricated magnetic lanthanum (La)-doped HAp nanoparticles/chitosan scaffolds (MLaHA/CS) capable of recruiting rat bone marrow mesenchymal stem cells (rBMSCs) and modulating host-to-scaffold immune responses through macrophage polarization, for bone regeneration. The scaffolds presented interconnected

macropores with plate-shaped nanoparticles and  $\approx 50$ – $150$  nm width and  $\approx 30$  nm thickness. It was observed that the magnetic nanoparticles and La dopants can inhibit the differentiation of macrophages toward M1, thus decreasing the inflammatory response and promotes M2 macrophage polarization, providing a pro-regenerative microenvironment for bone repair (Figure 12A). In vivo tests performed in rat calvarial defect mode showed high new bone formation in the MLaHA/CS group in comparison to the other compositions (Figure 12B).

Another interesting approach is the use of CaPs-based biomaterials to trigger desired immune responses and to enhance bone healing, mainly due to the osteoconductive capacity of CaPs.<sup>[129b,130]</sup> Furthermore, the CaPs structural features can strongly influence specific cell responses. For instance, nanoscale calcium deficient HAp (CDHA) can stimulate osteogenesis, while high porosity can positively modulate its inflammatory capability.<sup>[130d]</sup> Additionally, combining CaPs with MSCs highlight the main role of the host immune system for regeneration of bone.<sup>[129b]</sup> On the other hand,  $\beta$ -TCP seeded with macrophages presented reduced pro-inflammatory cytokines in comparison to CDHA biomaterial.<sup>[130a]</sup> Recently, scaffolding strategies comprising  $\beta$ -TCP functionalized with bioactive ions able to modulate the biological responses of bone have been proposed.<sup>[27d,35b,131]</sup> For instance, biocomposites made of  $\beta$ -TCP doped with  $Mn^{2+}$ ,  $Zn^{2+}$ , and/or  $Sr^{2+}$  in combination with SF presented biological responses according to the specific ionic dopant.<sup>[131]</sup> While  $Sr^{2+}$  and  $Mn^{2+}$  doping showed high osteogenesis, scaffolds doped with  $Zn^{2+}$  enhanced cell proliferation, thus showing capability of promoting immunomodulation.

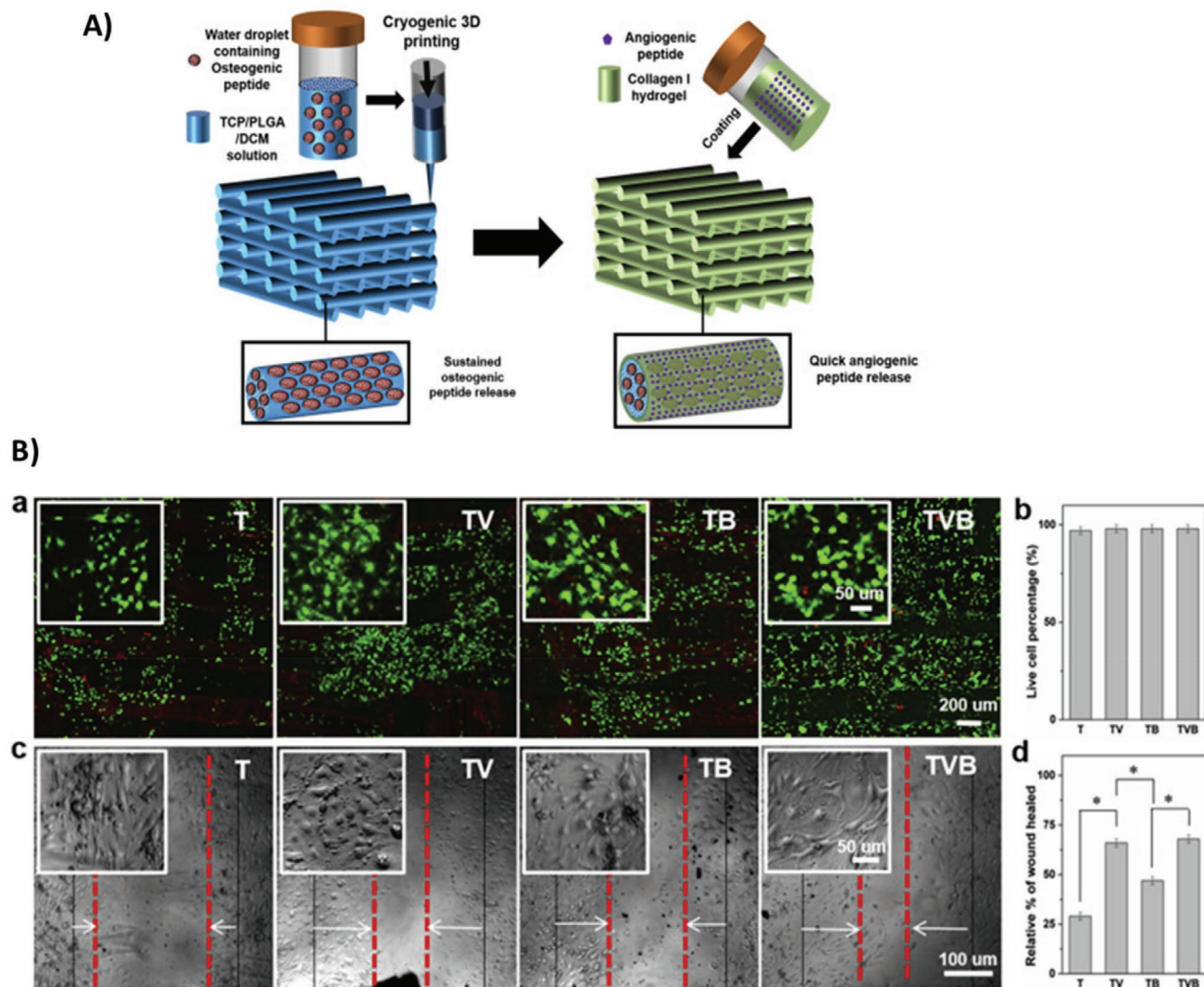


**Figure 10.** A) Schematic illustration of cryogenic 3D printing of TCP/PLGA/DCM containing osteogenic peptide (OP) and covered by angiogenic peptide (AP); B) Angiogenic study of the scaffolds: a,b) live and dead images of endothelial cells ECs on scaffolds and viability; c,d) EC migration of the scaffolds extracts after 12 h of culture. T: TCP/PLGA, TV: AP/collagen/TCP/PLGA, TB: OP/TCP/PLGA, TVB: AP/collagen/OP/TCP/PLG. Reproduced with permission.<sup>[104]</sup> Copyright 2021, Elsevier.

## 8. Conclusion and Future Perspectives

It is apparent that both traditional and state-of-the-art means of tissue engineering have potential in BTE. Optimal fabrication methods must be capable of producing a composite scaffold, which can meet the desired tissue characteristics (i.e., structural stability—porosity, pore size, and pore interconnectivity, mechanical properties, biocompatibility, osteoconductivity/osteogenicity, and angiogenesis potential), which is still a challenge. Only with attention to the relationship between these key characteristics and fabrication methodology will be possible to develop suitable biomaterials, with hierarchical structure identical to natural bone tissue.

While adaptation and realization of scaffold fabrication techniques for clinical translation of BTE remains a major challenge, with a very limited number of scaffolds being used

clinically. It is likely that scaffold fabrication methods using single material will not take the lead in BTE due to the complex composite nature of bone tissue. Since scaffold structural features heavily influence mechanical and biological properties, processing with random pore orientation and lack of pore control will become inappropriate for demanding applications, such as large bone replacement. Furthermore, it is now clear, that the incorporation of a controlled hierarchical pore structure, with interconnected pore networks of defined pore shape are critical for the fabrication of bone tissue. Therefore, scaffold fabrication will be focused on techniques which can control these elements.

Advances in magnetic resonance imaging (MRI), computed tomography (CT), and micro-CT scanning have led to the possibility of patient specific structural information, which can feedback into the scaffold design loop and be used



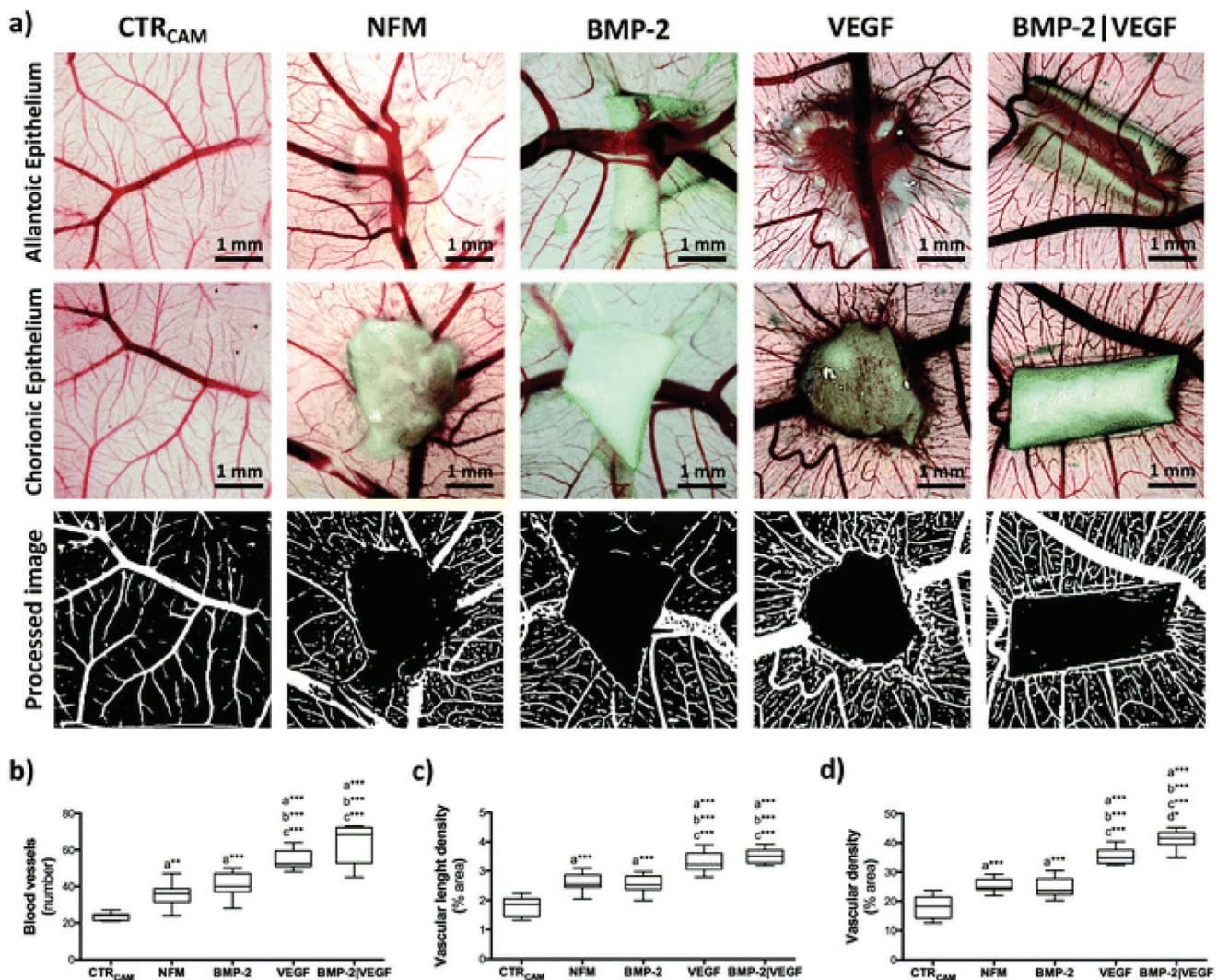


**Figure 11.** a) Representative photographs of ex ovo CAM after 7 days of implantation; b) Blood vessels quantification; c) Vascular length density (i.e., ratio of skeletonized vasculature area to total area); and d) Vascular density (i.e., ratio of vasculature area to total selection area). (\* $p < 0.01$ ; \*\* $p < 0.001$ ; \*\*\* $p < 0.0001$ ): *a* denotes significant differences compared to CTR<sub>CAM</sub>; *b* denotes significant differences compared to NFM; *c* denotes significant differences compared to BMP-2; *d* denotes significant differences compared to VEGF. Reproduced with permission.<sup>[118]</sup> Copyright 2020, Royal Society of Chemistry.

to monitor postoperative structural changes. In general, AM-based techniques are capable of closely producing desired scaffold architectures through the utilization of digital twins (CAD models). Currently, structural and resolution deficiencies across other techniques are attributed to physical limitations within the hardware. While this approach is still novel for techniques such as electrospinning, it highlights the benefit of the basic principles of AM-based approaches. However, controlling fiber diameter across complicated process-based interactions, such as whipping amplitude, electrostatic forces, and viscoelastic forces, remains problematic for electrospinning techniques.

Furthermore, combining CAD with statistical techniques and finite element analysis (FEA) can provide further insight into the relationship of structure and mechanical properties. While extrusion-based AM systems have the most promise to replicate constructs with predefined internal geometries, they are slow

and print resolutions are poor due to the physical limitations of the system (i.e., nozzle diameter and motion control). Overcoming these limitations will be critical for BTE to progress, candidate methodologies will likely include the combination of techniques. Cell viability and perfusion of nutrients throughout the full structure will require new bioinks with the incorporation of microcarriers showing promise. Polymerization-based fabrication methods (e.g., SLA) can overcome resolution and speed issues; however, new materials must be developed while considering their characteristics outlined herein. Among the collection of different biomaterials used in the scaffolds fabrication, the combination of polymers and inorganic materials are considered the most promising ones. These composite materials have better strength, adequate biodegradability, and immune response.

In brief, to create bone tissue which mimics the native ECM, further efforts are required in the area of structure-processing

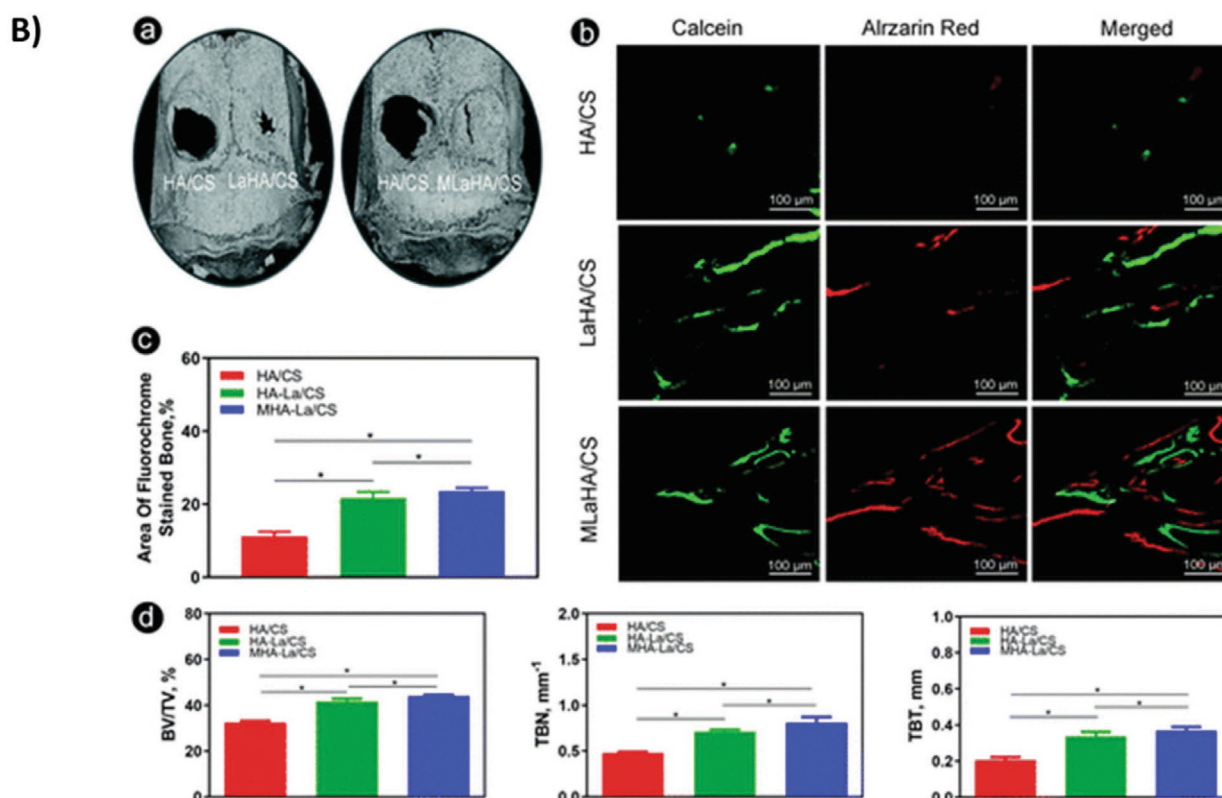
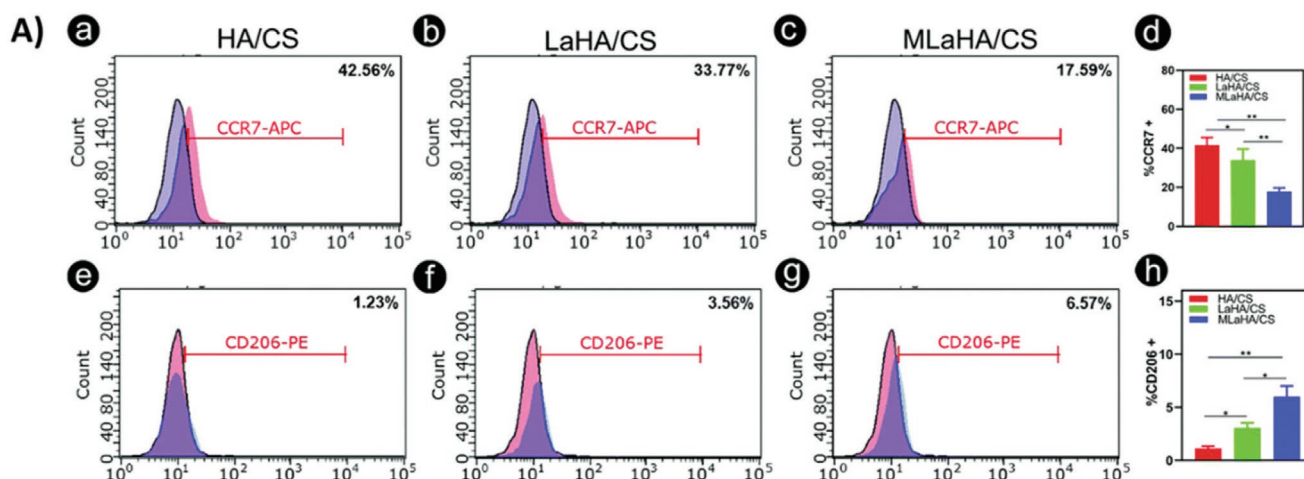


**Figure 12.** A) Detection of M1 and M2 polarization by flow cytometry with macrophages. B-a) Micro-CT analysis of calvarial bone defects after 9 weeks of implantation; b) New bone formation determined by fluorochrome-labeling analysis, including casein (green) at week 4 and Alizarin Red (red) at week 8; c) The percentages of fluorochrome areas ( $p < 0.05$ ); and d) BV/TV, TBN, TBT values in bone defect area ( $p < 0.05$ ). BV/TV: bone volume/total volume; TBT: bone trabecular thickness; TBN: bone trabecular number. HA/CS: HAP/chitosan scaffolds; LaHA/CS: La-doped HAP/chitosan scaffolds; MLaHA/CS: magnetic La-doped HAP/chitosan scaffolds. Reproduced with permission.<sup>[126c]</sup> Copyright 2020, Royal Society of Chemistry.

relationships with concurrent material development. Due to the inherent limitations mentioned regarding the different fabrication techniques, combined strategies offer potential. Additive manufacturing techniques linked with the latest medical imaging techniques offer vast potential over the coming years

to bring patient specific solutions from the lab to the bedside while offering improved patient outcomes.

Regarding the grand challenge of vascularization and immunomodulation in BTE, several approaches have been successfully reported to induce angiogenesis and osteogenesis.



However, effective application of tissue engineered vascularized bone grafts in clinics is very limited. Attention should be given to properly understand the kinetics of growth factors release and the local biomechanical environment. In this context, engineered gradients during scaffold development can open up new possibilities for BTE.

Finally, considerations should be placed on biomimetic scaffold design with incorporated immunomodulatory characteristics to enhance in situ bone regeneration for improved clinical outcomes.

## Acknowledgements

M.N.C. and G.R. contributed equally to this work. The authors thank the financial support from the Portuguese Foundation for Science and Technology for the funds provided under the distinctions attributed to J.M.O. (IF/01285/2015) and S.P. (CEECIND/03673/2017), and for the project 3BIOMED (ref. JICAM/0001/2017).

## Conflict of Interest

The authors declare no conflict of interest.

## Keywords

bioprinting, bones, electrospinning, immunomodulation, scaffolds, tissue engineering, vascularization

Received: December 9, 2020

Revised: January 26, 2021

Published online:

- [1] Research and Markets, Orthopedic Surgery-Global Trends & Opportunities, **2018**.
- [2] G. Turnbull, J. Clarke, F. Picard, P. Riches, L. Jia, F. Han, B. Li, W. Shu, *Bioact. Mater.* **2018**, *3*, 278.
- [3] D. Zhang, X. Wu, J. Chen, K. Lin, *Bioact. Mater.* **2018**, *3*, 129.
- [4] a) P. Feng, P. Wu, C. D. Gao, Y. W. Yang, W. Guo, W. J. Yang, C. J. Shuai, *Adv. Sci.* **2018**, *5*, 1700817; b) C. J. Shuai, Z. C. Zeng, Y. W. Yang, F. W. Qi, S. P. Peng, W. J. Yang, C. X. He, G. Y. Wang, G. W. Qian, *Mater. Des.* **2020**, *190*, 108564; c) S. Torgbo, P. Sukyai, *Appl. Mater. Today* **2018**, *11*, 34; d) W. Nie, C. Peng, X. J. Zhou, L. Chen, W. Z. Wang, Y. Z. Zhang, P. X. Ma, C. L. He, *Carbon* **2017**, *116*, 325; e) D. A. Osorio, B. E. J. Lee, J. M. Kwiecien, X. Y. Wang, I. Shahid, A. L. Hurley, E. D. Cranston, K. Grandfield, *Acta Biomater.* **2019**, *87*, 152; f) T. Xu, H. Y. Yang, D. Z. Yang, Z. Z. Yu, *ACS Appl. Mater. Interfaces* **2017**, *9*, 21094; g) C. Sharma, A. K. Dinda, P. D. Potdar, C. F. Chou, N. C. Mishra, *Mater. Sci. Eng., C* **2016**, *64*, 416.
- [5] H. Jodati, B. Yilmaz, Z. Evis, *Ceram. Int.* **2020**, *46*, 15725.
- [6] a) A. Wubneh, E. K. Tsekoura, C. Ayranci, H. Uludağ, *Acta Biomater.* **2018**, *80*, 1; b) H. D. Kim, S. Amirthalingam, S. L. Kim, S. S. Lee, J. Rangasamy, N. S. Hwang, *Adv. Healthcare Mater.* **2017**, *6*, 1700612; c) P. Chocholata, V. Kulda, V. Babuska, *Materials* **2019**, *12*, 568; d) M. N. Collins, C. Birkinshaw, *Carbohydr. Polym.* **2013**, *92*, 1262; e) J. Lim, M. L. You, J. Li, Z. B. Li, *Mater. Sci. Eng., C* **2017**, *79*, 917.
- [7] a) J. Melke, S. Midha, S. Ghosh, K. Ito, S. Hofmann, *Acta Biomater.* **2016**, *31*, 1; b) S. P. Soundarya, A. H. Menon, S. V. Chandran,

- N. Selvamurugan, *Int. J. Biol. Macromol.* **2018**, *119*, 1228;
- c) S. Saravanan, R. S. Leena, N. Selvamurugan, *Int. J. Biol. Macromol.* **2016**, *93*, 1354; d) D. Wang, J. Jang, K. Kim, J. Kim, C. B. Park, *Biomacromolecules* **2019**, *20*, 2684; e) S. Hassanajili, A. Karami-Pour, A. Oryan, T. Talaei-Khozani, *Mater. Sci. Eng., C* **2019**, *104*, 109960.
- [8] D. A. Taylor, L. C. Sampaio, Z. Ferdous, A. S. Gobin, L. J. Taite, *Acta Biomater.* **2018**, *74*, 74.
- [9] a) R. LogithKumar, A. KeshavNarayan, S. Dhivya, A. Chawla, S. Saravanan, N. Selvamurugan, *Carbohydr. Polym.* **2016**, *151*, 172; b) H. W. Qu, H. Y. Fu, Z. Y. Han, Y. Sun, *RSC Adv.* **2019**, *9*, 26252; c) G. L. Koons, M. Diba, A. G. Mikos, *Nat. Rev. Mater.* **2020**, *5*, 584; d) R. Eivazzadeh-Keihan, A. Maleki, M. de la Guardia, M. S. Bani, K. K. Chenab, P. Pashazadeh-Panahi, B. Baradaran, A. Mokhtarzadeh, M. R. Hamblin, *J. Adv. Res.* **2019**, *18*, 185; e) S. Chahal, A. Kumar, F. S. J. Hussian, *J. Biomater. Sci., Polym. Ed.* **2019**, *30*, 1308; f) D. P. Bhattarai, L. E. Aguilar, C. H. Park, C. S. Kim, *Membranes* **2018**, *8*, 62.
- [10] a) J. J. Li, M. Ebied, J. Xu, H. Zreiqat, *Adv. Healthcare Mater.* **2018**, *7*, 1701061; b) H. W. Qu, *Mater. Today Commun.* **2020**, *24*, 101024; c) A. P. M. Madrid, S. M. Vrech, M. A. Sanchez, A. P. Rodriguez, *Mater. Sci. Eng., C* **2019**, *100*, 631; d) X. Zhou, Y. H. Feng, J. H. Zhang, Y. B. Shi, L. Wang, *Int. J. Adv. Manuf. Technol.* **2020**, *108*, 3591.
- [11] a) Y. Wen, S. Xun, M. Haoye, S. Baichuan, C. Peng, L. Xuejian, Z. Kaihong, Y. Xuan, P. Jiang, L. Shibi, *Biomater. Sci.* **2017**, *5*, 1690; b) I. Denry, L. T. Kuhn, *Dent. Mater.* **2016**, *32*, 43; c) S. Gómez, M. Vlad, J. López, E. Fernández, *Acta Biomater.* **2016**, *42*, 341; d) X. Y. Zhang, G. Fang, J. Zhou, *Materials* **2017**, *10*, 50.
- [12] P. N. Christy, S. K. Basha, V. S. Kumari, A. Bashir, M. Maaza, K. Kaviyarasu, M. V. Arasu, N. A. Al-Dhabi, S. Ignacimuthu, *J. Drug Delivery Sci. Technol.* **2020**, *55*, 101452.
- [13] D. Sreenivasan, P. Tu, M. Dickinson, M. Watson, A. Blais, R. Das, J. Cornish, J. Fernandez, *Comput. Biol. Med.* **2016**, *68*, 9.
- [14] A. Barradas, H. Yuan, C. A. van Blitterswijk, P. Habibovic, *Eur. Cell Mater.* **2011**, *21*, 29.
- [15] C. A. Murphy, J. B. Costa, J. Silva-Correia, J. M. Oliveira, R. L. Reis, M. N. Collins, *Appl. Mater. Today* **2018**, *12*, 51.
- [16] A. Souness, F. Zamboni, G. M. Walker, M. N. Collins, *J. Biomed. Mater. Res. B* **2018**, *106*, 533.
- [17] S. Kuttappan, D. Mathew, M. B. Nair, *Int. J. Biol. Macromol.* **2016**, *93*, 1390.
- [18] a) P. A. Gunatillake, R. Adhikari, *Eur. Cell Mater.* **2003**, *5*, 1; b) N. A. S. Manssor, Z. Radzi, N. A. Yahya, L. M. Yusof, F. Hariri, N. H. Khairuddin, N. H. A. Kasim, J. T. Czernuszka, *Skin Pharmacol. Physiol.* **2016**, *29*, 55; c) S. P. Pilipchuk, A. B. Plonka, A. Monje, A. D. Taut, A. Lanis, B. Kang, W. V. Giannobile, *Dent. Mater.* **2015**, *31*, 317; d) L.-C. Gerhardt, A. R. Boccaccini, *Materials* **2010**, *3*, 3867; e) E. Novitskaya, P.-Y. Chen, E. Hamed, L. Jun, V. A. Lubarda, I. Jasiuk, J. McKittrick, *Theor. Appl. Mech.* **2011**, *38*, 209.
- [19] I. Matai, G. Kaur, A. Seyedsalehi, A. McClinton, C. T. Laurencin, *Biomaterials* **2019**, *226*, 119536.
- [20] M. S. Hasan, I. Ahmed, A. J. Parsons, C. D. Rudd, G. S. Walker, C. A. Scotchford, *J. Biomater. Appl.* **2013**, *28*, 354.
- [21] a) M.-P. Ginebra, M. Espanol, Y. Maazouz, V. Bergez, D. Pastorino, *EFORT Open Rev.* **2018**, *3*, 173; b) S. Torgbo, P. Sukyai, *Mater. Chem. Phys.* **2019**, *237*, 121868; c) L. Gritsch, M. Maqbool, V. Mouriño, F. E. Ciraldo, M. Cresswell, P. R. Jackson, C. Lovell, A. R. Boccaccini, *J. Mater. Chem. B* **2019**, *7*, 6109; d) P. Chen, L. Liu, J. Pan, J. Mei, C. Li, Y. Zheng, *Mater. Sci. Eng., C* **2019**, *97*, 325; e) I. K. Januariyasa, I. D. Ana, Y. Yusuf, *Mater. Sci. Eng., C* **2020**, *107*, 110347.
- [22] a) S. Kargozar, M. Montazerian, E. Fiume, F. Baino, *Front. Bioeng. Biotechnol.* **2019**, *7*, 161; b) X. Du, D. Wei, L. Huang, M. Zhu, Y. Zhang, Y. Zhu, *Mater. Sci. Eng., C* **2019**, *103*, 109731.
- [23] E. Kolos, A. Ruys, *Materials* **2015**, *8*, 3584.

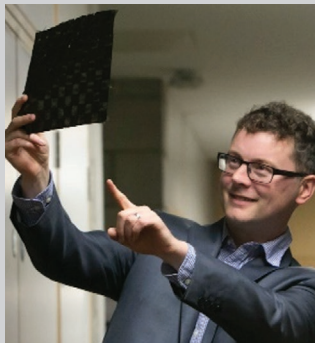
- [24] S. Pieralli, R. J. Kohal, R. E. Jung, K. Vach, B. C. Spies, *J. Dent. Res.* **2016**, *96*, 38.
- [25] S. Gorgieva, V. Kokol, in *Biomaterials Applications for Nanomedicine* (Ed: R. Pignatello), Intech Open, London, UK **2011**.
- [26] a) S. D. Purohit, R. Bhaskar, H. Singh, I. Yadav, M. K. Gupta, N. C. Mishra, *Int. J. Biol. Macromol.* **2019**, *133*, 592; b) I. E. Carlström, A. Rashad, E. Campodoni, M. Sandri, K. Syverud, A. I. Bolstad, K. Mustafa, *Mater. Lett.* **2020**, *264*, 127326; c) H.-T. Lu, T.-W. Lu, C.-H. Chen, F.-L. Mi, *Int. J. Biol. Macromol.* **2019**, *128*, 973; d) R. Mishra, R. Varshney, N. Das, D. Sircar, P. Roy, *Eur. Polym. J.* **2019**, *119*, 155.
- [27] a) B. Kundu, R. Rajkhowa, S. C. Kundu, X. Wang, *Adv. Drug Delivery Rev.* **2013**, *65*, 457; b) L. P. Yan, J. M. Oliveira, A. L. Oliveira, S. G. Caridade, J. F. Mano, R. L. Reis, *Acta Biomater.* **2012**, *8*, 289; c) L. Gambari, E. Amore, R. Raggio, W. Bonani, M. Barone, G. Lisignoli, B. Grigolo, A. Motta, F. Grassi, *Mater. Sci. Eng., C* **2019**, *102*, 471; d) V. P. Ribeiro, S. Pina, J. B. Costa, I. F. Cengiz, L. García-Fernández, *ACS Appl. Mater. Interfaces* **2019**, *11*, 3781.
- [28] a) R. H. Tammi, A. Kultti, V.-M. Kosma, R. Pirinen, P. Auvinen, M. I. Tammi, *Semin. Cancer Biol.* **2008**, *18*, 288; b) J. Gaffney, S. Matou-Nasri, M. Grau-Olivares, M. Slevin, *Mol. BioSyst.* **2010**, *6*, 437; c) P. Makvandi, G. W. Ali, F. D. Sala, W. I. Abdel-Fattah, A. Borzacchiello, *Mater. Sci. Eng., C* **2020**, *107*, 110195; d) Y. Zhou, Z. Gu, J. Liu, K. Huang, G. Liu, J. Wu, *Carbohydr. Polym.* **2020**, *230*, 115640.
- [29] a) S. S. Silva, J. F. Mano, R. L. Reis, *Crit. Rev. Biotechnol.* **2010**, *30*, 200; b) F. H. Tao, Y. X. Cheng, X. W. Shi, H. F. Zheng, Y. M. Du, W. Xiang, H. B. Deng, *Carbohydr. Polym.* **2020**, *230*, 115658; c) S. Ranganathan, B. Balagangadharan, N. Selvamurugan, *Int. J. Biol. Macromol.* **2019**, *133*, 354; d) L. Nie, Q. Wu, H. Long, K. Hu, P. Li, C. Wang, M. Sun, J. Dong, X. Wei, J. Suo, D. Hua, S. Liu, H. Yuan, S. Yang, *J. Biomater. Sci. Polym. Ed.* **2019**, *30*, 1636.
- [30] a) R. Chandrasekaran, R. P. Millane, S. Arnott, E. D. T. Atkins, *Carbohydr. Res.* **1988**, *175*, 1; b) S. Vieira, A. da Silva Moraes, E. Garet, J. Silva-Correia, R. L. Reis, Á. González-Fernández, J. M. Oliveira, *Acta Biomater.* **2019**, *93*, 74.
- [31] a) J. Sun, H. Tan, *Materials* **2013**, *6*, 1285; b) A. C. Hernandez-Gonzalez, L. Tellez-Jurado, L. M. Rodriguez-Lorenzo, *Carbohydr. Polym.* **2020**, *229*, 115514.
- [32] a) N. J. Gunja, K. A. Athanasiou, *Sports Med. Arthrosc.* **2006**, *14*, 112; b) J. Ju, X. Peng, K. Huang, L. Li, X. Liu, C. Chitrakar, L. Chang, Z. Gu, T. Kuang, *Polymer* **2019**, *180*, 121707; c) B. Ashwin, B. Abinaya, T. Prasith, S. V. Chandran, L. R. Yadav, M. Vairamani, S. Patil, N. Selvamurugan, *Int. J. Biol. Macromol.* **2020**, *162*, 523.
- [33] a) F. Donnalaja, E. Jacchetti, M. Soncini, M. T. Raimondi, *Polymers* **2020**, *12*, 905; b) A. Wibowo, C. Vyas, G. Cooper, F. Qulub, R. Suratman, A. I. Mahyuddin, T. Dirgantara, P. Bartolo, *Materials* **2020**, *13*, 512; c) D. Chuan, R. Fan, Y. Wang, Y. Ren, C. Wang, Y. Du, L. Zhou, J. Yu, Y. Gu, H. Chen, *Compos. Sci. Technol.* **2020**, *192*, 108107.
- [34] F. Ghorbani, A. Zamanian, A. Aidun, *J. Appl. Polym. Sci.* **2019**, *136*, 47656.
- [35] a) S. Pina, V. Ribeiro, R. L. Reis, O. J. M., *Patent number WO2018215997*, **2018**; b) V. P. Ribeiro, S. Pina, R. F. Canadas, A. d. S. Moraes, C. Vilela, S. Vieira, I. F. Cengiz, R. L. Reis, J. M. Oliveira, *Regener. Med. Front.* **2019**, *1*, e190007; c) P.-Y. Yun, Y.-K. Kim, K.-I. Jeong, J.-C. Park, Y.-J. Choi, *J. Cranio-Maxillofac. Surg.* **2014**, *42*, 1909; d) M. Shaltoolki, G. Dini, M. Mehdikhani, *Mater. Sci. Eng., C* **2019**, *105*, 110138; e) W. Wang, J. R. P. Junior, P. R. L. Nalesso, D. Musson, J. Cornish, F. Mendonça, G. F. Caetano, P. Bártole, *Mater. Sci. Eng., C* **2019**, *100*, 759; f) C. Gayer, J. Ritter, M. Bullemer, S. Grom, L. Jauer, W. Meiners, A. Pfister, F. Reinauer, M. Vučák, K. Wissenbach, *Mater. Sci. Eng., C* **2019**, *101*, 660; g) B. Bochicchio, K. Barbaro, A. De Bonis, J. V. Rau, A. Pepe, *J. Biomed. Mater. Res., Part A* **2020**, *108*, 1064.
- [36] A. J. Salinas, M. Vallet-Regi, *RSC Adv.* **2013**, *3*, 11116.
- [37] a) S. Wang, L. Liu, K. Li, L. Zhu, J. Chen, Y. Hao, *Mater. Des.* **2019**, *168*, 107643; b) W. Xu, J. Tian, Z. Liu, X. Lu, M. D. Hayat, Y. Yan, Z. Li, X. Qu, C. Wen, *Mater. Sci. Eng., C* **2019**, *105*, 110015.
- [38] R. G. Ribas, V. M. Schatkoski, T. L. do Amaral Montanheiro, B. R. C. de Menezes, C. Stegemann, D. M. G. Leite, G. P. Thim, *Ceram. Int.* **2019**, *45*, 21051.
- [39] S. M. Kurtz, S. Kocagöz, C. Arnholt, R. Huet, M. Ueno, W. L. Walter, *J. Mech. Behav. Biomed.* **2014**, *31*, 107.
- [40] a) K. D. Lobel, L. L. Hench, *J. Sol-Gel Sci. Technol.* **1996**, *7*, 69; b) A. A. Gorustovich, J. A. Roether, A. R. Boccaccini, *Tissue Eng., Part B* **2010**, *16*, 199; c) I. D. Xynos, A. J. Edgar, L. D. K. Buttery, L. L. Hench, J. M. Polak, *Biochem. Biophys. Res. Commun.* **2000**, *276*, 461.
- [41] a) S. Bose, N. Sarkar, *Trends Biotechnol.* **2020**, *38*, 404; b) M. Pang, Y. Huang, F. Meng, Y. Zhuang, H. Liu, M. Du, Q. Ma, Q. Wang, Z. Chen, L. Chen, *Eur. Polym. J.* **2020**, *122*, 109365.
- [42] Z.-H. Li, S.-C. Ji, Y.-Z. Wang, X.-C. Shen, H. Liang, *Front. Mater. Sci.* **2013**, *7*, 237.
- [43] S. Pina, J. M. Oliveira, R. L. Reis, *Adv. Mater.* **2015**, *27*, 1143.
- [44] A. Cahyanto, K. Tsuru, K. Ishikawa, M. Kikuchi, in *Multifunctional Bioceramics for Innovative Therapy*, Trans Tech Publications Ltd., Switzerland **2017**, pp. 167–172.
- [45] A. M. Ferreira, P. Gentile, V. Chiono, G. Ciardelli, *Acta Biomater.* **2012**, *8*, 3191.
- [46] J.-K. Cho, Y.-G. Jin, S.-J. Rha, S.-J. Kim, J.-H. Hwang, *Food Chem.* **2014**, *159*, 200.
- [47] M. Echave, P. Sánchez, J. Pedraz, G. Orive, *J. Drug Delivery Sci. Technol.* **2017**, *42*, 63.
- [48] K. Su, C. Wang, *Biotechnol. Lett.* **2015**, *37*, 2139.
- [49] D. Wilson, R. Valluzzi, D. Kaplan, *Biophys. J.* **2000**, *78*, 2690.
- [50] X. Z. Shu, Y. Liu, F. Palumbo, G. D. Prestwich, *Biomaterials* **2003**, *24*, 3825.
- [51] R. C. F. Cheung, T. B. Ng, J. H. Wong, W. Y. Chan, *Mar. Drugs* **2015**, *13*, 5156.
- [52] a) J. Silva-Correia, J. M. Oliveira, R. L. Reis, in *Biomaterials from Nature for Advanced Devices and Therapies* (Eds.: N. M. Neves, R. L. Reis), Wiley, Hoboken, NJ **2016**, p. 320; b) L. R. Stevens, K. J. Gilmore, G. G. Wallace, M. in het Panhuis, *Biomater. Sci.* **2016**, *4*, 1276.
- [53] a) B. Raphael, T. Khalil, V. L. Workman, A. Smith, C. P. Brown, C. Streuli, A. Saiani, M. Domingos, *Mater. Lett.* **2017**, *190*, 103; b) A. Asti, L. Gioglio, *Int. J. Artif. Organs* **2014**, *37*, 187.
- [54] C. Holten, *Lactic Acid: Properties and Chemistry of Lactic Acid and Derivatives*, Verlag Chemie, Weinheim **1971**.
- [55] D. Cohn, H. Younes, G. Marom, *Polymer* **1987**, *28*, 2018.
- [56] a) I. Engelberg, J. Kohn, *Biomaterials* **1991**, *12*, 292; b) A. A. Deshpande, J. Heller, R. Gurny, *Crit. Rev. Ther. Drug Carrier Syst.* **1998**, *154*, 381; c) R. S. Bezwada, D. D. Jamiolkowski, L. In-Young, V. Agarwal, J. Persivale, S. Trenka-Benthin, M. Erneta, J. Suryadevara, A. Yang, S. Liu, *Biomaterials* **1995**, *16*, 1141.
- [57] H. L. Khor, K. W. Ng, J. T. Schantz, T. T. Phan, T. C. Lim, S. H. Teoh, D. W. Hutmacher, *Mater. Sci. Eng., C* **2002**, *20*, 71.
- [58] a) D. Cohn, T. Stern, M. F. Gonzalez, J. Epstein, *J. Biomed. Mater. Res.* **2002**, *59*, 273; b) M. A. Woodruff, D. W. Hutmacher, *Prog. Polym. Sci.* **2010**, *35*, 1217; c) D. Gorth, T. J. Webster, in *Biomaterials for Artificial Organs*, Woodhead Publishing, Cambridge **2011**; d) P. Gentile, V. Chiono, I. Carmagnola, P. V. Hatton, *Int. J. Mol. Sci.* **2014**, *15*, 3640; e) J. C. Middleton, A. J. Tipton, *Biomaterials* **2000**, *21*, 2335; f) T. Gredes, S. Schönitz, T. Gedrange, L. Stepien, K. Kozak, C. Kunert-Keil, *Biomater. Res.* **2017**, *21*, 8.
- [59] a) F. Wu, C. Liu, B. O'Neill, J. Wei, Y. Ngothai, *Appl. Surf. Sci.* **2012**, *258*, 7589; b) F. Zamboni, M. Keays, S. Hayes, A. B. Albadarin, G. M. Walker, P. A. Kiely, M. N. Collins, *Int. J. Pharm.* **2017**, *532*, 595.

- [60] a) J. M. Oliveira, M. T. Rodrigues, S. S. Silva, P. B. Malafaya, M. E. Gomes, C. A. Viegas, I. R. Dias, J. T. Azevedo, J. F. Mano, R. L. Reis, *Biomater* **2006**, *27*, 6123; b) L. P. Yan, J. Silva-Correia, C. Correia, S. G. Caridade, E. M. Fernandes, R. A. Sousa, J. F. Mano, J. M. Oliveira, A. L. Oliveira, R. L. Reis, *Nanomedicine* **2013**, *8*, 359; c) L.-P. Yan, J. Silva-Correia, M. B. Oliveira, C. Vilela, H. Pereira, R. A. Sousa, J. F. Mano, A. L. Oliveira, J. M. Oliveira, R. L. Reis, *Acta Biomater.* **2015**, *12*, 227; d) R. Canadas, D. Pereira, J. Silva-Correia, A. Marques, J. Oliveira, R. Reis, *J. Tissue Eng. Regen. Med.* **2012**, *6*, 8.
- [61] D. Dehnad, Z. Emam-Djomeh, H. Mirzaei, S.-M. Jafari, S. Dadashi, *Carbohydr. Polym.* **2014**, *105*, 222.
- [62] a) S. L. Feng, F. P. He, J. D. Ye, *Mater. Sci. Eng., C* **2018**, *82*, 217; b) D. X. Ke, S. Bose, *Addit. Manuf.* **2018**, *22*, 111; c) X. N. Chen, H. Y. Fan, X. W. Deng, L. N. Wu, T. Yi, L. X. Gu, C. C. Zhou, Y. J. Fan, X. D. Zhang, *Nanomaterials* **2018**, *8*, 960; d) S. W. Chen, Q. Zhang, T. Nakamoto, N. Kawazoe, G. P. Chen, *Tissue Eng., Part C* **2016**, *22*, 189.
- [63] a) D. Chimene, L. Miller, L. M. Cross, M. K. Jaiswal, I. Singh, A. K. Gaharwar, *ACS Appl. Mater. Interfaces* **2020**, *12*, 15976; b) W. Kim, G. Kim, *Biofabrication* **2020**, *12*, 015007; c) S. M. Bittner, J. L. Guo, A. G. Mikos, *Bioprinting* **2018**, *12*, e00e00032; d) T. M. De Witte, L. E. Fratila-Apachitei, A. A. Zadpoor, N. A. Peppas, *Regen. Biomater.* **2018**, *5*, 197; e) S. Azizian, A. Hadjizadeh, H. Niknejad, *Carbohydr. Polym.* **2018**, *202*, 315; f) D. Qu, J. P. Zhu, H. R. Childs, H. H. Lu, *Acta Biomater.* **2019**, *93*, 111.
- [64] a) T. L. Lu, Y. H. Li, T. Chen, *Int. J. Nanomed.* **2013**, *8*, 337; b) A. Haider, S. Haider, M. R. Kummar, T. Kamal, A.-A. A. Alghyamah, F. J. Iftikhar, B. Bano, N. Khan, M. A. Afridi, S. S. Han, *J. Saudi Chem. Soc.* **2020**, *24*, 186; c) A. Eltom, G. Y. Zhong, A. Muhammad, *Adv. Mater. Sci. Eng.* **2019**, *2019*, 3429527.
- [65] a) A. Prasad, M. R. Sankar, V. Katiyar, *Mater. Today Proc.* **2017**, *4*, 898; b) M. S. Khoramgah, J. Ranjbari, H. A. Abbaszadeh, F. S. T. Mirakabad, S. Hatami, S. Hosseinzadeh, H. Ghanbarian, *Bioimpacts* **2020**, *10*, 73.
- [66] a) L. Zhang, G. J. Yang, B. N. Johnson, X. F. Jia, *Acta Biomater.* **2019**, *84*, 16; b) A. Haleem, M. Javaid, R. H. Khan, R. Suman, *J. Clin. Orthop. Trauma* **2020**, *11*, S118; c) S. Bose, C. Koski, A. A. Vu, *Mater. Horiz.* **2020**, *7*, 2011; d) L. Piaia, G. V. Salmoria, D. Hotza, *Mater. Res.* **2020**, *23*; e) M. Orciani, M. Fini, R. Di Primio, M. Mattioli-Belmonte, *Front. Bioeng. Biotechnol.* **2017**, *5*, 17.
- [67] C. Shen, L. Witek, R. L. Flores, N. Tovar, A. Torroni, P. G. Coelho, F. K. Kasper, M. Wong, S. Young, *Tissue Eng., Part A* **2020**, *26*, 1303.
- [68] A. D. Bagde, A. M. Kuthe, S. Quazi, V. Gupta, S. Jaiswal, S. Jyothilal, N. Lande, S. Nagdeve, *Irbm* **2019**, *40*, 133.
- [69] a) A. C. Daly, F. E. Freeman, T. Gonzalez-Fernandez, S. E. Critchley, J. Nulty, D. J. Kelly, *Adv. Healthcare Mater.* **2017**, *6*, 1700298; b) T. Genova, I. Roato, M. Carossa, C. Motta, D. Cavagnetto, F. Mussano, *Int. J. Mol. Sci.* **2020**, *21*, 7012; c) A. Leucht, A. C. Volz, J. Rogal, K. Borchers, P. J. Kluger, *Sci. Rep.* **2020**, *10*, 5330; d) M. A. Kuss, R. Harms, S. H. Wu, Y. Wang, J. B. Untrauer, M. A. Carlson, B. Duan, *RSC Adv.* **2017**, *7*, 29312; e) M. Askari, M. A. Naniz, M. Kouhi, A. Saberi, A. Zolfagharian, M. Bodaghi, *Biomater. Sci.* **2021**, *9*, 535.
- [70] J. White, M. Foley, A. Rowley, *3D Print. Addit. Manuf.* **2015**, *2*, 145.
- [71] Y. E. Arslan, T. S. Arslan, B. Derkus, E. Emregul, K. C. Emregul, *Colloids Surf., B* **2017**, *154*, 160.
- [72] T. D. Ngo, A. Kashani, G. Imbalzano, K. T. Nguyen, D. Hui, *Composites, Part B* **2018**, *143*, 172.
- [73] a) B. Zhang, L. Gao, L. Ma, Y. Luo, H. Yang, Z. Cui, *Engineering* **2019**, *5*, 777; b) S. Pina, V. P. Ribeiro, C. F. Marques, F. R. Maia, T. H. Silva, R. L. Reis, J. M. Oliveira, *Materials* **2019**, *12*, 1824; c) E. Sodupe-Ortega, A. Sanz-Garcia, A. Pernia-Espinoza, C. Escobedo-Lucea, *Materials* **2018**, *11*, 1402.
- [74] E. S. Bishop, S. Mostafa, M. Pakvasa, H. H. Luu, M. J. Lee, J. M. Wolf, G. A. Ameer, T. C. He, R. R. Reid, *Genes Dis.* **2017**, *4*, 185.
- [75] D. Chimene, K. K. Lennox, R. R. Kaunas, A. K. Gaharwar, *Ann. Biomed. Eng.* **2016**, *44*, 2090.
- [76] W. Hu, Z. Wang, Y. Xiao, S. Zhang, J. Wang, *Biomater. Sci.* **2019**, *7*, 843.
- [77] A. GhavamiNejad, N. Ashammakhi, X. Y. Wu, A. Khademhosseini, *Small* **2020**, *16*, 2002931.
- [78] M. Ermis, S. Calamak, G. Calibas Kocal, S. Guven, N. G. Durmus, I. Rizvi, T. Hasan, N. Hasirci, V. Hasirci, U. Demirci, in *Handbook of Nanomaterials for Cancer Theranostics* (Ed: J. Conde), Elsevier, Amsterdam **2018**, p. 463.
- [79] M. Khanmohammadi, M. B. Dastjerdi, A. Ai, A. Ahmadi, A. Godarzi, A. Rahimi, J. Ai, *Biomater. Sci.* **2018**, *6*, 1286.
- [80] N. C. Veitch, A. T. Smith, in *Advances in Inorganic Chemistry*, Vol. 51, Academic Press, Cambridge, MA **2000**, p. 107.
- [81] J. B. Costa, J. Silva-Correia, J. M. Oliveira, R. L. Reis, *Adv. Healthc. Mater.* **2017**, *6*, 1701021.
- [82] J. Jang, J. Y. Park, G. Gao, D.-W. Cho, *Biomaterials* **2018**, *156*, 88.
- [83] I. T. Ozbolat, *Trends Biotechnol.* **2015**, *33*, 395.
- [84] A. Ovsianikov, A. Khademhosseini, V. Mironov, *Trends Biotechnol.* **2018**, *36*, 348.
- [85] a) F. Fahimipour, E. Dashtimoghdam, M. M. Hasani-Sadrabadi, J. Vargas, D. Vashae, D. C. Lobner, T. S. J. Kashi, B. Ghasemzadeh, L. Tayebi, *Dent. Mater.* **2019**, *35*, 990; b) M. Whitely, S. Cereceres, P. Dhavalikar, K. Salhadar, T. Wilems, B. Smith, A. Mikos, E. Cosgriff-Hernandez, *Biomaterials* **2018**, *185*, 194; c) D. Seliktar, *Science* **2012**, *336*, 1124; d) E. Prince, E. Kumacheva, *Nat. Rev. Mater.* **2019**, *4*, 99.
- [86] S. V. Murphy, A. Skardal, A. Atala, *J. Biomed. Mater. Res., Part A* **2013**, *101*, 272.
- [87] a) J. B. Costa, J. Park, A. M. Jorgensen, J. Silva-Correia, R. L. Reis, J. M. Oliveira, A. Atala, J. J. Yoo, S. J. Lee, *Chem. Mater.* **2020**, *32*, 8733; b) X. Z. Li, J. Chen, Z. Xu, Q. Zou, L. Yang, M. X. Ma, L. P. Shu, Z. X. He, C. Ye, *J. Mater. Sci.: Mater. Med.* **2020**, *31*, 13; c) G. Ratheesh, C. Vaquette, Y. Xiao, *Adv. Healthcare Mater.* **2020**, *9*, 2001323.
- [88] a) *Tissue Eng., Part C* **2019**, *25*, 276; b) J. Lee, J. Hong, W. Kim, G. H. Kim, *Carbohydr. Polym.* **2020**, *250*, 116914; c) C. Suhun, S. Yucheng, C. Yeong-Jin, H. Dong-Heon, J. In-Ho, C. Dong-Woo, *Biofabrication* **2020**; d) F. E. Freeman, D. C. Browe, J. Nulty, S. Von Euw, W. L. Grayson, D. J. Kelly, *Eur. Cell Mater.* **2019**, *38*, 168.
- [89] a) A. Gilpin, Y. Yang, *Biomed Res. Int.* **2017**, *2017*, 9831534; b) Y. Hashimoto, S. Funamoto, T. Kimura, K. Nam, T. Fujisato, A. Kishida, *Biomaterials* **2011**, *32*, 7060.
- [90] E. G. Santoso, K. Yoshida, Y. Hirota, M. Aizawa, O. Yoshino, A. Kishida, Y. Osuga, S. Saito, T. Ushida, K. S. Furukawa, *PLoS One* **2014**, *9*, e103201.
- [91] T. Hoshiba, T. Yamaoka, in *Decellularized Extracellular Matrix: Characterization, Fabrication and Applications*, The Royal Society of Chemistry, London **2020**, p. 1.
- [92] a) B. Kim, R. Ventura, B. T. Lee, *Macromol. Biosci.* **2018**, *18*, 1800025; b) R. Junka, X. Yu, *Mater. Sci. Eng., C* **2020**, *113*, 110981; c) J. Y. Kim, G. Ahn, C. Kim, J. S. Lee, I. G. Lee, S. H. An, W. S. Yun, S. Y. Kim, J. H. Shim, *Macromol. Biosci.* **2018**, *18*, e1800025.
- [93] A. R. Amini, C. T. Laurencin, S. P. Nukavarapu, *Crit. Rev. Biomed. Eng.* **2012**, *40*, 363.
- [94] L. Roseti, V. Parisi, M. Petretta, C. Cavallo, G. Desando, I. Bartolotti, B. Grigolo, *Mater. Sci. Eng., C* **2017**, *78*, 1246.
- [95] H. J. Haugen, S. P. Lyngstadaas, F. Rossi, G. Perale, *J. Clin. Periodontol.* **2019**, *46*, 92.
- [96] N. Abbasi, S. Hamlet, R. M. Love, N.-T. Nguyen, *J. Sci.: Adv. Mater. Devices* **2020**, *5*, 1.
- [97] Y. Yan, H. Chen, H. Zhang, C. Guo, K. Yang, K. Chen, R. Cheng, N. Qian, N. Sandler, Y. S. Zhang, *Biomaterials* **2019**, *190*, 97.



- [98] M. J. Gupte, W. B. Swanson, J. Hu, X. Jin, H. Ma, Z. Zhang, Z. Liu, K. Feng, G. Feng, G. Xiao, *Acta Biomater.* **2018**, *82*, 1.
- [99] C. Ghayor, F. E. Weber, *Front. Physiol.* **2018**, *9*, 960.
- [100] S. Derakhshanfar, R. Mbeleck, K. G. Xu, X. Y. Zhang, W. Zhong, M. Xing, *Bioact. Mater.* **2018**, *3*, 144.
- [101] A. A. Ezhilarasi, J. J. Vijaya, K. Kaviyarasu, L. J. Kennedy, R. J. Ramalingam, H. A. Al-Lohedan, *J. Photochem. Photobiol., B* **2018**, *180*, 39.
- [102] R. A. Perez, J.-E. Won, J. C. Knowles, H.-W. Kim, *Adv. Drug Delivery Rev.* **2013**, *65*, 471.
- [103] A. Hasan, G. Waibhaw, V. Saxena, L. M. Pandey, *Int. J. Biol. Macromol.* **2018**, *111*, 923.
- [104] a) Z. Wang, A. Hui, H. Zhao, X. Ye, C. Zhang, A. Wang, C. Zhang, *Int. J. Nanomed.* **2020**, *15*, 6945; b) M. R. Bidgoli, I. Alemzadeh, E. Tamjid, M. Khafaji, M. Vossoughi, *Mater. Sci. Eng., C* **2019**, *103*, 109688; c) Y. Gu, J. Zhang, X. Zhang, G. Liang, T. Xu, W. Niu, *Tissue Eng. Regener. Med.* **2019**, *16*, 415; d) Y.-H. A. Wu, Y.-C. Chiu, Y.-H. Lin, C.-C. Ho, M.-Y. Shie, Y.-W. Chen, *Int. J. Mol. Sci.* **2019**, *20*, 942; e) C. Wang, W. Huang, Y. Zhou, L. He, Z. He, Z. Chen, X. He, S. Tian, J. Liao, B. Lu, *Bioact. Mater.* **2020**, *5*, 82; f) C. Wang, J. H. Lai, K. Li, S. K. Zhu, B. H. Lu, J. Liu, Y. J. Tang, Y. Wei, *Bioact. Mater.* **2021**, *6*, 137; g) H. A.-D. M. Abu Awwad, L. Thiagarajan, J. M. Kanczler, M. H. Amer, G. Bruce, S. Lanham, R. M. H. Rumney, R. O. C. Oreffo, J. E. Dixon, *J. Controlled Release* **2020**, *325*, 335.
- [105] a) Y. S. Kim, M. Majid, A. J. Melchiorri, A. G. Mikos, *Bioeng. Transl. Med.* **2018**, *4*, 83; b) M. Parmaksiz, A. E. Elçin, Y. M. Elçin, *Mater. Sci. Eng., C* **2019**, *94*, 788.
- [106] M. Hospodiuk, M. Dey, D. Sosnoski, I. T. Ozbolat, *Biotechnol. Adv.* **2017**, *35*, 217.
- [107] J.-H. Zeng, S.-W. Liu, L. Xiong, P. Qiu, L.-H. Ding, S.-L. Xiong, J.-T. Li, X.-G. Liao, Z.-M. Tang, *J. Orthop. Surg. Res.* **2018**, *13*, 33.
- [108] a) T. Lou, X. Wang, G. Song, Z. Gu, Z. Yang, *Int. J. Biol. Macromol.* **2014**, *69*, 464; b) Y. W. Chen, Y. F. Shen, C. C. Ho, J. Yu, Y. H. A. Wu, K. Wang, C. T. Shih, M. Y. Shie, *Mater. Sci. Eng., C* **2018**, *91*, 679.
- [109] J. S. Lee, H. D. Cha, J. H. Shim, J. W. Jung, J. Y. Kim, D. W. Cho, *J. Biomed. Mater. Res., Part A* **2012**, *100*, 1846.
- [110] A. Arora, A. Kothari, D. S. Katti, *J. Mech. Behav. Biomed.* **2015**, *57*, 169.
- [111] C. Zhou, K. Yang, K. Wang, X. Pei, Z. Dong, Y. Hong, X. Zhang, *Mater. Des.* **2016**, *109*, 415.
- [112] J.-A. Kim, J. Lim, R. Naren, H.-s. Yun, E. K. Park, *Acta Biomater.* **2016**, *44*, 155.
- [113] Y. Liu, S. Yang, L. Cao, X. Zhang, J. Wang, C. Liu, *Mater. Sci. Eng., C* **2020**, *110*, 110622.
- [114] J.-p. Zheng, L.-j. Chen, D.-y. Chen, C.-s. Shao, M.-f. Yi, B. Zhang, *Trans. Nonferrous Met. Soc. China* **2019**, *29*, 2534.
- [115] a) Á. E. Mercado-Pagán, A. M. Stahl, Y. Shanjani, Y. Yang, *Ann. Biomed. Eng.* **2015**, *43*, 718; b) P. Carmeliet, *Nat. Med.* **2003**, *9*, 653.
- [116] B. Decker, H. Bartels, S. Decker, *Anat. Rec.* **1995**, *242*, 310.
- [117] A. Grosso, M. G. Burger, A. Lunger, D. J. Schaefer, A. Banfi, N. Di Maggio, *Front Bioeng. Biotechnol.* **2017**, *5*, 68.
- [118] a) S. Yin, W. Zhang, Z. Zhang, X. Jiang, *Adv. Healthcare Mater.* **2019**, *8*, 1801433; b) Y. J. He, S. Lin, Q. Ao, X. N. He, *Stem Cell Res. Ther.* **2020**, *11*, 12; c) M. R. Casanova, C. Oliveira, E. M. Fernandes, R. L. Reis, T. H. Silva, A. Martins, N. M. Neves, *Biomater. Sci.* **2020**, *8*, 2577; d) D. Mitra, J. Whitehead, O. W. Yasui, J. K. Leach, *Biomaterials* **2017**, *146*, 29; e) B. Divband, M. Samiei, S. Davaran, L. Roshangar, S. Shahi, M. Aghazadeh, *Biointerface Res. Appl. Chem.* **2021**, *11*, 8043.
- [119] A. Marrella, T. Y. Lee, D. H. Lee, S. Karuthedom, D. Syla, A. Chawla, A. Khademhosseini, H. L. Jang, *Mater. Today* **2018**, *21*, 362.
- [120] a) L. M. Ma, S. Cheng, X. F. Ji, Y. Zhou, Y. S. Zhang, Q. T. Li, C. H. Tan, F. Peng, Y. Zhang, W. H. Huang, *Mater. Sci. Eng., C* **2020**, *117*, 111303; b) Z. Y. Xu, Y. L. Xu, P. Basuthakur, C. R. Patra, S. Ramakrishna, Y. Liu, V. Thomas, H. S. Nanda, *J. Mater. Chem. B* **2020**, *8*, 9110; c) C. Stahli, M. James-Bhasin, A. Hoppe, A. R. Boccaccini, S. N. Nazhat, *Acta Biomater.* **2015**, *19*, 15; d) S. N. Rath, A. Brandl, D. Hiller, A. Hoppe, U. Gbureck, R. E. Horch, A. R. Boccaccini, U. Kneser, *PLoS One* **2014**, *9*, 24.
- [121] a) K. Hu, B. R. Olsen, *Bone* **2016**, *91*, 30; b) Y. Bai, G. Yin, Z. Huang, X. Liao, X. Chen, Y. Yao, X. Pu, *Int. Immunopharmacol.* **2013**, *16*, 214.
- [122] a) M. Honda, R. Hariya, M. Matsumoto, M. Aizawa, *Materials* **2019**, *12*, 2068; b) G. Thrivikraman, A. Athirasala, R. Gordon, L. Zhang, R. Bergan, D. R. Keene, J. M. Jones, H. Xie, Z. Chen, J. Tao, B. Wingender, L. Gower, J. L. Ferracane, L. E. Bertassoni, *Nat. Commun.* **2019**, *10*, 3520; c) M. Markou, D. Kouroupis, F. Badounas, A. Katsouras, A. Kyrkou, T. Fotsis, C. Murphy, E. Bagli, *Front. Bioeng. Biotechnol.* **2020**, *8*, 278.
- [123] a) K. Glenske, P. Donkiewicz, A. Kówitsch, N. Milosevic-Oljaca, P. Rider, S. Rofall, J. Franke, O. Jung, R. Smeets, R. Schnettler, S. Wensch, M. Barbeck, *Int. J. Mol. Sci.* **2018**, *19*, 826; b) M. M. Martino, S. Brkic, E. Bovo, M. Burger, D. J. Schaefer, T. Wolff, L. Gürke, P. S. Briquez, H. M. Larsson, R. Gianni-Barrera, J. A. Hubbell, A. Banfi, *Front. Bioeng. Biotechnol.* **2015**, *3*, 45; c) F. Shahabipour, N. Ashammakhi, R. K. Osukee, S. Bonakdar, T. Hoffman, M. A. Shokrgozar, A. Khademhosseini, *Transl. Res.* **2020**, *216*, 57; d) A. Piroso, R. Gottardi, P. G. Alexander, R. S. Tuan, *Stem Cell Res. Ther.* **2018**, *9*, 112.
- [124] T. H. Qazi, J. C. Berkman, J. Schoon, S. Geißler, G. N. Duda, A. R. Boccaccini, E. Lippens, *J. Biomed. Mater. Res., Part A* **2018**, *106*, 2827.
- [125] A. Hoppe, N. S. Güldal, A. R. Boccaccini, *Biomaterials* **2011**, *32*, 2757.
- [126] a) C. Wang, B. Chen, W. Wang, X. Zhang, T. Hu, Y. He, K. Lin, X. Liu, *Mater. Sci. Eng., C* **2019**, *103*, 109833; b) A. H. Lourenço, A. L. Torres, D. P. Vasconcelos, C. Ribeiro-Machado, J. N. Barbosa, M. A. Barbosa, C. C. Barrias, C. C. Ribeiro, *Mater. Sci. Eng., C* **2019**, *99*, 1289; c) Q. Wang, Y. Tang, Q. Ke, W. Yin, C. Zhang, Y. Guo, J. Guan, *J. Mater. Chem. B* **2020**, *8*, 5280.
- [127] J. Lee, H. Byun, S. K. M. Perikamana, S. Lee, H. Shin, *Adv. Healthcare Mater.* **2019**, *8*, 1800861.
- [128] a) F. Zamboni, S. Vieira, R. L. Reis, J. M. Oliveira, M. N. Collins, *Prog. Mater. Sci.* **2018**, *97*, 97; b) F. Zamboni, E. Ryan, M. Culebras, M. N. Collins, *Carbohydr. Polym.* **2020**, *245*, 116501.
- [129] a) J. I. Andorko, C. M. Jewell, *Bioeng. Transl. Med.* **2017**, *2*, 139; b) P. Humbert, M. Brennan, N. Davison, P. Rosset, V. Trichet, F. Blanchard, P. Layrolle, *Front. Immunol.* **2019**, *10*, 663.
- [130] a) J. M. Sadowska, F. Wei, J. Guo, J. Guillem-Marti, Z. Lin, M. P. Ginebra, Y. Xiao, *Acta Biomater.* **2019**, *96*, 605; b) T. Li, M. Peng, Z. Yang, X. Zhou, Y. Deng, C. Jiang, M. Xiao, J. Wang, *Acta Biomater.* **2018**, *71*, 96; c) I. Kurzina, Y. Churina, Y. Shapovalova, V. Syusyukina, J. Kzhyshkowska, *Bioceram. Dev. Appl.* **2018**, *8*, 109; d) J. M. Sadowska, F. Wei, J. Guo, J. Guillem-Marti, M.-P. Ginebra, Y. Xiao, *Biomaterials* **2018**, *181*, 318.
- [131] S. Pina, R. F. Canadas, G. Jiménez, M. Perán, J. A. Marchal, R. L. Reis, J. M. Oliveira, *Cells Tissues Organs* **2017**, *204*, 150.





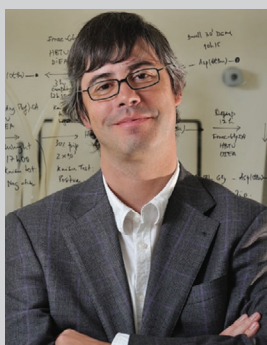
**Maurice N. Collins** is a materials scientist. He is a senior lecturer at the School of Engineering, principal investigator at the Bernal Institute, the Health Research Institute, and funded investigator at the AMBER center, at the University of Limerick, in Ireland. He is the course director of biomedical device materials M.Sc. and leads a lab on biomedical and sustainable polymers. His research is focused on the structure/property/processing relationships of polymeric materials and how these influence the function. Current areas of interest include: hydrogels, 3D bioprinting, sustainable carbon materials (carbon fibers, nanofibers, and nanocarriers), immunomodulatory, and animate materials for a variety of biomedical applications.



**Guang Ren** is a postdoctoral researcher at Dr. Maurice Collins's laboratory of the Bernal Institute, University of Limerick. He received a B.Eng. in Materials Engineering at Wuhan University of Technology in 2010, an M.Sc. in Advanced Materials, and a Ph.D. in Materials Science at the University of Limerick in 2012 and 2019, respectively. Dr. Guang Ren's research focuses on bio-based materials, biomedical materials, 3D printing techniques, and interconnect materials for microelectronic applications.



**Sandra Pina** is an assistant researcher at the 3B's Research Group on Biomaterials, Biodegradables, and Biomimetics (a member of the ICVS/3B's Associate Laboratory), University of Minho. Her research has been focusing on the field of bioresorbable bioceramics (calcium phosphate-based materials) and biocomposites for tissue engineering and regeneration with main applications in bone and osteochondral tissue. In addition, she has been developing different ion-doped materials with great potential for being used in MRI (cell tracking and biodistribution studies) and immunomodulation.



**Rui L. Reis** is the Vice-President for R&D of the University of Minho, Portugal, Director of the 3B's Research Group and the ICVS/3B's Associate Laboratory of UMinho. He is CEO of the European Institute of Excellence on Tissue Engineering and Regenerative Medicine. His main area of research is the development of biomaterials from natural origin polymers for bone replacement and fixation, drug delivery carriers, and tissue engineering scaffolding for different tissues. He is an FBSE, FTERM, and NAE member. He was awarded an ERC Advanced Grant, ESAFORM 2001 Scientific Prize, JeanLeRay Award 2002, Stimulus to Excellence Award 2004.



**J. Miguel Oliveira** is a principal investigator and Vice-President of Institute 3Bs, University of Minho, PT. He is also Director of Pre-Clinical Research at the Porto - FIFA Medical Center, PT. His research interest includes biomaterials for tissue engineering, nanomedicine, stem cells engineering, and cell/drug delivery applications. Over the years, he has focused his research activities on the development of complex in vitro models. He has been awarded several prizes, including the Jean Leray Award 2015.